SECURITY INFORMATION

CONFIDENTIAL RESTRICTED

256

RM L51J08

NACA RM L51J08

NACA

CASE FILE COPY

RESEARCH MEMORANDUM

EFFECT OF VERTICAL LOCATION OF A HORIZONTAL TAIL ON THE STATIC LONGITUDINAL STABILITY CHARACTERISTICS OF A 45° SWEPTBACK-WING - FUSELAGE COMBINATION OF ASPECT RATIO 8 AT A REYNOLDS NUMBER OF 4.0×10^6

By Reino J. Salmi and William A. Jacques

Langley Aeronautical Laboratory
Langley Field, Va.

CLASSIFICATION CHANGED TO UNCLASSIFIED CLASSIFICATION CHANGED TO CONFIDENTIAL

AUTHORITY: NACA RESEARCH ABSTRACT NO. W99 CROWLEY CHANGE #1605 DATE 12-1-53 T.C.F.

DATE: APRIL 13, 1956 WHL

CLASSIFIED DOCUMENT

This material contains information affecting the National Defense of the United States within the meaning of the espionage laws, Title 18, U.S.C., Secs. 793 and 794, the transmission or revelation of which in any manner to unauthorized person is prohibited by law.

NATIONAL ADVISORY COMMITTEE FOR AERONAUTICS

WASHINGTON

January 21, 1952

CONFIDENTIAL RESTRICTED

NATIONAL ADVISORY COMMITTEE FOR AERONAUTICS

RESEARCH MEMORANDUM

EFFECT OF VERTICAL LOCATION OF A HORIZONTAL TAIL ON THE STATIC LONGITUDINAL STABILITY CHARACTERISTICS OF A 45° SWEPTBACK-WING - FUSELAGE COMBINATION OF ASPECT RATIO 8 AT A REYNOLDS NUMBER OF 4.0×10^6

By Reino J. Salmi and William A. Jacques

SUMMARY

An experimental investigation of the effects of a horizontal tail in various vertical positions on the longitudinal stability characteristics of a wing-fuselage combination of 45° sweepback and aspect ratio 8 was made in the Langley 19-foot pressure tunnel. The tests were made at two wing incidence angles and with various high-lift and stall-control devices at a Reynolds number of 4.0×10^6 and a Mach number of 0.19. The horizontal tail was tested at four vertical positions.

The results of the investigation indicated that the stabilizing influence of the tail varied with the distance of the tail from the extended wing-chord plane in a manner similar to that obtained on previous investigations of sweptback-wing models of lower aspect ratio; that is, the tail effectiveness through the high lift-coefficient range increased when the tail was located just below the extended wing-chord plane, but as the tail height above the wing-chord plane was increased, the tail effectiveness decreased through the high lift-coefficient range. At the highest position tested, the tail was destabilizing in the high lift-coefficient range. As a result of large improvements in the stability in the high lift-coefficient range obtained with leading-edge flaps and fences, favorable over-all pitching-moment characteristics were obtained through the high lift-coefficient range with and without trailing-edge flaps when the tail was located -0.060 semispan below the extended wing-chord plane, and only small unstable variations were obtained with a tail height of 0.140 semispan.

INTRODUCTION

The design information necessary to evaluate optimum configurations for high-subsonic-speed long-range airplanes has been extended to include a 45° sweptback wing of aspect ratio 8 (references 1 and 2). This wing is in a previously unexplored aspect-ratio range for highly sweptback wings.

Previous investigations of sweptback-wing configurations (references 3 and 4) have shown that the effectiveness of a horizontal tail is influenced greatly by the vertical position of the horizontal tail relative to the wing wake. It was also indicated that the increase in the effectiveness of a horizontal tail at high lift coefficients, when it is located in the proper position, can be advantageously used to counteract the inherent instability of highly sweptback-wing - fuselage configurations of moderate and large aspect ratios.

The present investigation was made, therefore, to determine the low-speed static longitudinal stability characteristics of the 45° sweptback wing of aspect ratio 8 in combination with a fuselage and a horizontal tail. The tests were made at a Reynolds number of 4.0×10^6 and a Mach number of 0.19 for four tail positions and various flap and stall-control configurations.

SYMBOLS

C_L lift coefficient $\left(\frac{\text{Lift}}{qS}\right)$

C_m pitching-moment coefficient about $0.25\bar{c}$ $\left(\frac{\text{Pitching moment}}{qS\bar{c}}\right)$

S wing area

S_t tail area

$\bar{c}$ mean aerodynamic chord $\left(\frac{2}{S}\int_0^{b/2} c^2 dy\right)$

c wing chord

b	wing span
y	lateral distance from plane of symmetry
q	free-stream dynamic pressure $\left(\frac{1}{2}\rho V^2\right)$
ρ	mass density of air
V	free-stream velocity
q_t	dynamic pressure at tail
ϵ	downwash angle, degrees
α	angle of attack of wing
α_t	angle of attack of tail
$\frac{dC_m}{dC_L}$	rate of change of pitching-moment coefficient with lift coefficient
$\frac{d\epsilon}{d\alpha}$	rate of change of downwash angle with angle of attack
τ	tail effectiveness parameter $\left(\frac{dC_{m_t}/d\alpha}{\frac{S_t}{S}\frac{l}{\bar{c}}C_{L_{\alpha_t}}}\right)$
$\frac{dC_{m_t}}{d\alpha}$	rate of change of pitching moment due to tail with angle of attack
$C_{L_{\alpha_t}}$	lift-curve slope of isolated tail, 0.055 per degree
l	tail length, distance from $0.25\bar{c}$ of wing to $0.25\bar{c}$ of tail
$C_{m_{i_t}}$	rate of change of pitching moment with tail incidence angle
$\left(C_{m_{i_t}}\right)_0$	value of $C_{m_{i_t}}$ at zero wing lift

i_w wing incidence angle referred to fuselage center line, positive when trailing edge is down

i_t tail incidence angle referred to wing-chord plane, positive when trailing edge is down

$i_{t(trim)}$ tail incidence angle required for zero pitching moment

z tail height, measured normal to wing-chord plane

η tail efficiency factor, ratio of $\left(C_{m_{i_t}}\right)_0$ of any tail position to $\left(C_{m_{i_t}}\right)_0'$

$\left(C_{m_{i_t}}\right)_0'$ $\left(C_{m_{i_t}}\right)_0$ for high tail position $\left(z = 0.300 \frac{b}{2}\right)$ with wing flaps neutral and $\alpha = 0^\circ$

Subscripts:

e effective value, based on force data

t tail

max maximum

MODEL

The geometric characteristics of the model are shown in figures 1 and 2. The wing was swept back 45° at the quarter-chord line and had an aspect ratio of 8. The wing was constructed of a steel core with an outer layer consisting of an alloy of bismuth and tin, which was contoured to provide NACA 63_1A012 airfoil sections parallel to the plane of symmetry. The wing had no twist or dihedral. The circular fuselage was made from laminated mahogany and was finished with lacquer. Interchangeable fuselage blocks allowed the wing to be set at either 0° or 4° incidence.

The horizontal tail was swept back 45° at the quarter-chord line and had an aspect ratio of 4.0. The tail was machined from aluminum to provide NACA 63_1A012 sections parallel to the plane of symmetry. The tail was mounted on the fuselage by means of a thin steel post.

The leading-edge and trailing-edge flaps and the wing fences were made from sheet steel and mahogany. Details of the flaps and fences and their locations are shown in figure 2.

TESTS

The tests were conducted in the Langley 19-foot pressure tunnel with the air compressed to approximately 33.5 pounds per square inch, absolute. The data were obtained at Reynolds numbers of 4.0×10^6 with a corresponding Mach number of 0.19. Figure 3 shows the model mounted on the three-support system in the tunnel.

The aerodynamic forces and moments were measured through an angle-of-attack range from -2° to 30° for the various combinations tested. The tests were made at two values of wing incidence. For 0° wing incidence, tail heights of 4.5-percent and 14.0-percent semispan from the extended wing-chord plane were used. For 4° incidence of the wing, tail heights of -6.0-percent, 14.0-percent, and 30.0-percent semispan were tested (see fig. 4). The tail was tested at incidence angles of approximately 0°, -4°, and -8° for all tail positions, and in the case of $z = -6.0$-percent semispan, an additional tail incidence angle of -12° was tested. The tests were made for various combinations of leading-edge flaps, split flaps, and fences. Figure 5 may be used as a guide to the various combinations tested.

As an aid to subsequent analysis of the data, the tail was tested independently at a Reynolds number of 2.26×10^6 which corresponds to a wing Reynolds number of 4.0×10^6.

REDUCTION OF DATA

The data presented herein have been reduced to standard nondimensional form and have been corrected for air-stream misalinement, support tare and interference effects, and jet-boundary effects. The jet-boundary corrections to the angle of attack and pitching-moment coefficient were obtained by the method of reference 5.

Effective values of downwash angle and dynamic-pressure ratio.- The usual method of computing the effective downwash angle (reference 3) was not suitable because of the nonlinear lift curve of the isolated tail (fig. 6). The data were obtained at three and, in some cases, four tail

incidence angles. The pitching moment due to the tail C_{m_t} was plotted against the tail incidence angle i_t for various values of the wing angle of attack α. The intersection of the faired points with the C_{m_t} zero axis indicated the tail incidence angle for which the tail angle of attack was zero. The effective downwash angle ϵ_e was then obtained from the relation $\epsilon_e = \alpha + i_t - \alpha_t$.

Some values of the effective dynamic-pressure ratio at the tail $\left(q_t/q\right)_e$ which are based on the variation of the pitching moment coefficient with tail incidence angle $C_{m_{i_t}}$ were obtained. However, the values of $\left(q_t/q\right)_e$ were not considered to be of sufficient accuracy to warrant presentation. The tare due to the rear model support varied with changes in the tail incidence angle, thereby influencing $C_{m_{i_t}}$, but only an average tare was applied. An examination of the data indicated, however, that the influence of the tare was negligible in the determination of ϵ_e.

Tail-efficiency parameter.- The tail-efficiency parameter η represents the effective change in the lift-curve slope of the tail due to the effects of fuselage interference. The values of η are based on the variation of $C_{m_{i_t}}$ at zero wing lift for the various tail positions. The value of η was assumed to be 100 percent for the position 0.300b/2 above the extended wing-chord plane, inasmuch as the distance from the fuselage was large and the interference effects of the tail post would be very small. The values of η are also based on the assumption that the variation of q_t/q at zero wing lift with the flaps neutral was very small in the region of the tail. The value of η was obtained from the relation

$$\eta = \frac{\left(C_{m_{i_t}}\right)_0}{\left(C_{m_{i_t}}\right)_0'} \tag{1}$$

where the prime refers to the value for the high tail position. The values of $\left(C_{m_{i_t}}\right)_0$ used, which were averaged from the values obtained from the

configurations with the flaps neutral, with and without fences, are given in the following table:

Tail height, z	i_w (deg)	$\left(C_{m_{i_t}}\right)_0$	η (percent)
0.300b/2	4	-0.0270	100
.140b/2	4	-.0251	93
.140b/2	0	-.0262	97
.045b/2	0	-.0251	93
-.060b/2	4	-.0265	98

The effect of wing incidence angle on the tail-efficiency parameter (as determined at zero lift) was negligible, since the distance from the fuselage to the tail was the same for the 0.045b/2 $\left(i_w = 0^\circ\right)$ and the 0.140b/2 $\left(i_w = 4^\circ\right)$ tail positions, both of which had the same efficiency.

Tail effectiveness parameter.- The effectiveness of the tail can be conveniently expressed by the factor τ (reference 4), which accounts for the effects of the downwash-angle variation, the dynamic-pressure ratio, and the tail efficiency. The factor τ is defined as follows:

$$\tau = -\eta\left[\left(1 - \frac{d\epsilon}{d\alpha}\right)\frac{q_t}{q} + \alpha_t \frac{d\left(q_t/q\right)}{d\alpha}\right] \tag{2}$$

or

$$\tau = \frac{dC_{m_t}/d\alpha}{\frac{S_t}{S}\frac{l}{\bar{c}}C_{L_{\alpha_t}}} \approx \frac{\left(dC_{m_t}/d\alpha\right)_{measured}}{0.0264} \tag{3}$$

A negative value of τ indicates that the tail is contributing to the stability.

From equation 2 it can be seen that for finite values of α_t, τ is affected by the variation of q_t/q with α. Since a fairly large number of tail incidence angles were tested, τ was determined for $\alpha_t = 0$ up to a fairly high wing angle of attack. It is believed, however, that even at the very high angles of attack the effects of $\frac{d(q_t/q)}{d\alpha}$ are small and in any case do not affect the trends in the variations of τ with α.

Determination of dC_m/dC_L for $C_m = 0$.- For each model configuration tested, a family of curves of C_m plotted against C_L, for which the tail incidence angle was the parameter, was obtained from the basic data. In order to obtain values of dC_m/dC_L for $C_m = 0$ throughout the lift-coefficient range, the following procedure was used at those lift coefficients where the original data curves did not intersect the $C_m = 0$ axis. At any desired lift coefficient the value of dC_m/dC_L was measured from each of the original data curves and plotted against the corresponding value of C_m. These points were joined by a faired curve and the value of dC_m/dC_L for $C_m = 0$ for the desired lift coefficient was then read from the point where the faired curve crossed the $C_m = 0$ axis. In some cases a slight extrapolation of the faired curve was made.

RESULTS AND DISCUSSION

Method of Analysis

In the subsequent discussion, the effects of the tail on the longitudinal stability characteristics are explained by the variation of the tail-effectiveness parameter τ. An increase in τ will refer to an increase in value of the negative quantity - that is, an increase in the tail effectiveness.

As pointed out in reference 6, the slope of the curve of C_m plotted against C_L, (dC_m/dC_L), for the trimmed condition $C_m = 0$, is a valid measure of the static longitudinal stability. In the present case, it was preferable to use dC_m/dC_L for $C_m = 0$ rather than the neutral point, because accurate calculation of the neutral point in the high lift range was not feasible.

The variations of dC_m/dC_L for $C_m = 0$ for the tail-on configurations and dC_m/dC_L for the wing-fuselage combination are presented in figure 7 as functions of the lift coefficient for the various configurations tested. Figure 8 presents the variation of the tail effectiveness parameter τ and the downwash angle ϵ_e with angle of attack. The lift and pitching-moment characteristics are given in figure 9, and the variation with lift of the tail trim incidence angle is presented in figure 10.

Effect of Tail Height on the Longitudinal

Stability and on the Tail Effectiveness

Flaps neutral.- The plain wing-fuselage combination became unstable at a very low lift coefficient, as indicated by the positive values of dC_m/dC_L (fig. 7(a)), and increased in instability as the lift coefficient was increased. At lift coefficients greater than 1.0, dC_m/dC_L rapidly approached infinite values. The large positive increase in dC_m/dC_L above a lift coefficient of 1.0 ($\alpha = 18^\circ$) was not appreciably reduced by the tail, although the variation of the tail effectiveness parameter τ with angle of attack (fig. 8(a)) indicated an increase in the stabilizing influence of the tail at angles of attack greater than about 26° for all except the highest tail positions investigated. Figure 8(a) indicates that a general increase in the tail effectiveness with angle of attack throughout the angle-of-attack range was obtained for the low tail position $\left(z = -0.060 \frac{b}{2}\right)$. Figure 7(a) shows that the tail reduced slightly the forward movement of the aerodynamic center, as indicated by dC_m/dC_L, throughout the angle-of-attack range. The increase in the effectiveness of the tail in the low position reflects the decrease in $d\epsilon/d\alpha$, as indicated by the curves of ϵ_e against α. The favorable downwash variation may occur in the region below the wake center line, as indicated by references 3 and 4. When the tail was located 0.045b/2 or 0.140b/2 above the wing-chord plane, $d\epsilon/d\alpha$ increased slightly through the angle-of-attack range; whereas for a tail height of 0.300b/2, $d\epsilon/d\alpha$ exhibited a sharp increase at angles of attack above 20°, which caused the high tail to become destabilizing.

Upper-surface fences only.- Reference 2 indicated that the most favorable locations for upper-surface fences were at 0.575b/2 and 0.800b/2. A comparison of figures 7(a) and 7(b) indicated that the fences improved considerably the stability in the lift-coefficient range below 1.0 but did not prevent the increase of dC_m/dC_L to large positive values in the lift coefficient range above 1.0. Figures 8(a) and 8(b) indicate that the fences had a negligible effect on the tail effectiveness and on the downwash characteristics. Therefore, as in the case of the plain wing, the instability near the maximum lift coefficient was not satisfactorily reduced by the tail.

Leading-edge flaps and fences.- The data for the configurations with both 0.45b/2 leading-edge flaps and fences were obtained with the inboard fence located at 0.475b/2 instead of 0.575b/2. Comparative tests made with the 0.45b/2 leading-edge flaps on and the tail off indicated that only small differences occurred in the pitching-moment characteristics

between the two configurations. As indicated by the variation of dC_m/dC_L in figure 7(c), the stability throughout the lift-coefficient range was greatly improved by the combination of 0.45b/2 leading-edge flaps and fences. A comparison of figures 8(a) and 8(c) indicated that, in general, the combination of leading-edge flaps and fences improved the variation of τ with angle of attack in the angle-of-attack range below 20° but reduced the effectiveness above 20°. A favorable variation of dC_m/dC_L was obtained throughout the lift range for the low tail $\left(z = -0.060 \frac{b}{2}\right)$ in spite of the decrease in τ above 20° angle of attack (which corresponds to a wing lift coefficient of about 1.24), because the tail-off combination exhibited such a marked increase in stability at lift coefficients above 1.2 (fig. 7(c)).

Leading-edge and trailing-edge flap combinations.- The effects of the tail on the configurations with 0.35b/2 split flaps and 0.45b/2 leading-edge flaps were investigated with and without the wing fences.

The addition of 0.35b/2 split flaps to the wing with 0.45b/2 leading-edge flaps and fences improved the stability characteristics through most of the lift range, as shown by a comparison of figures 7(c) and 7(d), except for a large forward movement of the aerodynamic center which occurred at the maximum lift coefficient for the tail-off configuration. From a comparison of figures 8(c) and 8(d), it can be seen that the effect of the 0.35b/2 split flaps on the variation of the tail-effectiveness parameter was not consistent when the tail position was changed. In general, the 0.35b/2 split flaps tended to reduce the effectiveness in the moderately high angle-of-attack range (near 16°), except for the tail located in the -0.060b/2 position, and increase the effectiveness of the tail at very high angles of attack. From the variation of the pitching moment with angle of attack for the tail-off combination (fig. 9(d)), it can be seen that, although figure 7(d) indicates large positive values of dC_m/dC_L at $C_{L_{max}}$, the actual increase in pitching-moment coefficient was small, and, as a result, favorable over-all stability characteristics, as indicated by dC_m/dC_L in figure 7(d), were obtained with the tail in either the -0.060b/2 or 0.045b/2 positions. Although the high tail $\left(z = 0.300 \frac{b}{2}\right)$ was destabilizing in the high lift-coefficient range, the combination with the tail in the 0.140b/2 position, which is well above the wing-chord plane, exhibited only small unstable variations in dC_m/dC_L.

Figures 8(d) and 8(e) indicate that, except for the increases in τ in the high angle-of-attack range for the 0.140b/2 and 0.300b/2 tail positions, the removal of the fences did not appreciably affect the

variation of the tail effectiveness with angle of attack. As shown in figures 7(d) and 7(e) the forward movement of the aerodynamic center, as indicated by dC_m/dC_L, was greater for the tail-off combination with the fences off in the lift-coefficient range below $C_{L_{max}}$. The over-all stability characteristics for the 0.35b/2 split flaps and 0.45b/2 leading-edge flaps configuration with the tail on were, therefore, less desirable with the fences off than with the fences on, except for the lift-coefficient range near $C_{L_{max}}$.

The tail was also tested in conjunction with the wing-fuselage combination incorporating 0.50b/2 extended split flaps, 0.45b/2 leading-edge flaps and fences because of the interest in the greater lift obtainable with the 0.50b/2 extended split flaps, as shown by figures 9(b) and 9(f) and in reference 2. A comparison of figures 7(d) and 7(f) indicated that only minor differences in the stability characteristics throughout the lift range for both the tail-off and tail-on combinations resulted from the change in the trailing-edge flap configuration. Figures 8(d) and 8(f) indicate that the change in the split flaps to a greater span and a more rearward position tended to increase the tail effectiveness in the high angle-of-attack range, except for the high tail position, but did not change the trends in the variations of τ with angle of attack.

It may be of interest to note that for various configurations tested, the variations of τ reflected the changes in $d\epsilon/d\alpha$. Inasmuch as reference 1 indicates that the inboard sections do not stall, it is conjectured that the loss of dynamic pressure in the region of the tail for the present wing would not be very large.

Effect of wing incidence angle.- The effect of wing incidence angle on the tail effectiveness was determined for the tail in the 0.140b/2 position. The results indicated that, in general, the tail effectiveness in the major portion of the high angle-of-attack range (below 24°) was somewhat lower for a wing incidence angle of 0° than for 4° (fig. 8). Although the tail was further from the fuselage at zero wing incidence and had a greater efficiency at zero angle of attack, the wake interference effects of the fuselage through most of the high angle-of-attack range may have been greater.

General comments.- The results of the present investigation corroborate those of previous investigations (for example, see references 3 and 4) in that the tail position below the extended wing-chord plane exhibited the greatest effectiveness in the high lift range and the tail position well above the extended wing-chord plane was destabilizing in the high lift range.

The present investigation was limited in scope, since only one tail plan form and only a few tail positions were tested. However, the results indicated that although the low tail exhibited the greatest effectiveness in the high lift range, the small unstable variations for the tail just above the wing-chord plane may not be too severe to control. The tail positions above the wing-chord plane may be more desirable from high-speed considerations and also from the design standpoint. In the present case, the tail appeared to be somewhat more favorable in the 0.140b/2 position $\left(i_w = 4^\circ\right)$ than in the 0.045b/2 position $\left(i_w = 0^\circ\right)$ in that smaller unstable variations of the pitching moment were obtained.

Variation of tail trim incidence angle with lift.- The significance of unstable variations in the pitching-moment characteristics is probably more evident from the variation with lift coefficient of the tail incidence angle required for trim. When the rate of change of $i_{t(trim)}$ with lift coefficient $\frac{di_{t(trim)}}{dC_L}$ is negative, it indicates that a desirable variation in the stick position with lift coefficient will result - that is, a pull-back on the stick would be necessary to obtain a higher lift coefficient. Figure 10(a) indicates that a favorable variation of $i_{t(trim)}$ with lift coefficient was obtained up to a value of C_L of 1.0 for all tail positions for the configuration with fences only, whereas the plain wing $\frac{di_{t(trim)}}{dC_L}$ became positive at lift coefficients greater than about 0.55. When the leading-edge flaps and fences were on, $\frac{di_{t(trim)}}{dC_L}$ was negative throughout the lift range regardless of the trailing-edge flap configuration for tail heights of -0.060b/2 and 0.140b/2 $\left(i_w = 4^\circ\right)$, as indicated in figures 10(b) and 10(c). With the wing incidence angle at zero, however, the tail exhibited small undesirable variations in $i_{t(trim)}$ prior to the maximum lift coefficient for the 0.045b/2 and 0.140b/2 positions. For the high tail $\left(z = 0.300\ \frac{b}{2}\right)$, the undesirable variation of the trim incidence angle prior to the maximum lift was considerably greater than for the tail in the 0.045b/2 and 0.140b/2 positions. Where comparable flap configurations were tested with and without fences, the data indicated that removal of the fences increased the magnitude of any undesirable changes in the variation of $i_{t(trim)}$ with lift coefficient.

It may be of interest to note that when the 0.50b/2 extended split flaps are deflected, with the 0.45b/2 leading-edge flaps and fences on, a positive change in the tail incidence angle of over 6.5° is required for trim (fig. 10(c)). The large positive trim incidence change is required because most of the lift increase from the 0.50 extended split flaps is ahead of the wing center of gravity.

CONCLUSIONS

The following conclusions are based on an investigation of the effects of horizontal-tail location on the static longitudinal stability characteristics of a 45° sweptback-wing - fuselage combination of aspect ratio 8:

1. The tail effectiveness varied with the distance of the tail from the extended wing-chord plane in a manner similar to that obtained in previous investigations on sweptback-wing models of lower aspect ratio. The tail exhibited the greatest effectiveness in the moderate and high lift-coefficient range in the position -0.060 semispan below the extended wing-chord plane. In general, the tail effectiveness at high lift coefficients decreased as the tail was raised, and at the highest position tested (0.300 semispan above the extended wing-chord plane) the tail was destabilizing at high lift coefficients.

2. Although the effectiveness of the tail in the low position increased with angle of attack, it was insufficient to reduce appreciably the unstable changes due to the wing at a lift coefficient of about 0.55. The upper-surface wing fences had little effect on the tail effectiveness regardless of the wing-flap configuration. The fences delayed the instability due to the wing to a lift coefficient of about 1.00, but even with the fences on, the instability beyond a lift coefficient of 1.00 was too great to be reduced appreciably by the tail.

3. With both the leading-edge flaps and fences on the wing, the stability characteristics of the wing were improved to such an extent that favorable over-all pitching-moment characteristics throughout the lift range were obtained with the tail located -0.060 semispan below the extended wing-chord plane. Except for the high tail position, the leading-edge flaps tended to reduce the tail effectiveness at very high angles of attack.

4. In general, the addition of trailing-edge flaps increased the effectiveness of the tail at high lift coefficients for all the positions tested. The stability characteristics with the leading-edge flaps, trailing-edge flaps, and fences were favorable throughout the lift range

with the tail in the -0.060-semispan position. For the tail located in the 0.045-semispan and 0.140-semispan positions, small unstable variations occurred prior to the maximum lift. On the basis of the variation of the tail incidence required for trim, the -0.060-semispan and 0.140-semispan tail heights were the most favorable.

5. The stabilizing influence of the tail located 0.140 semispan from the extended wing-chord plane with the wing incidence angle at zero was generally less through the major portion of the high angle-of-attack range than when the tail was located 0.140 semispan from the wing-chord plane with the wing incidence at 4°.

Langley Aeronautical Laboratory
National Advisory Committee for Aeronautics
Langley Field, Va.

REFERENCES

1. Graham, Robert R.: Low-Speed Characteristics of a 45° Sweptback Wing of Aspect Ratio 8 from Pressure Distributions and Force Tests at Reynolds Numbers from 1,500,000 to 4,800,000. NACA RM L51H13, 1951.

2. Pratt, George L., and Shields, E. Rousseau: Low-Speed Longitudinal Characteristics of a 45° Sweptback Wing of Aspect Ratio 8 with High-Lift and Stall-Control Devices at Reynolds Numbers from 1,500,000 to 4,800,000. NACA RM L51J04, 1951.

3. Salmi, Reino J.: Horizontal-Tail Effectiveness and Downwash Surveys for Two 47.7° Sweptback Wing-Fuselage Combinations with Aspect Ratios of 5.1 and 6.0 at a Reynolds Number of 6.0×10^{6}. NACA RM L50K06, 1951.

4. Foster, Gerald V., and Griner, Roland F.: A Study of Several Factors Affecting the Stability Contributed by a Horizontal Tail at Various Vertical Positions on a Sweptback-Wing Airplane Model. NACA RM L9H19, 1949.

5. Sivells, James C., and Salmi, Rachel M.: Jet-Boundary Corrections for Complete and Semispan Swept Wings in Closed Circular Wind Tunnels. NACA TN 2454, 1951.

6. Kayten, Gerald G.: Analysis of Wind-Tunnel Stability and Control Tests in Terms of Flying Qualities of Full-Scale Airplanes. NACA Rep. 825, 1945. (Formerly NACA ARR 3J22.)

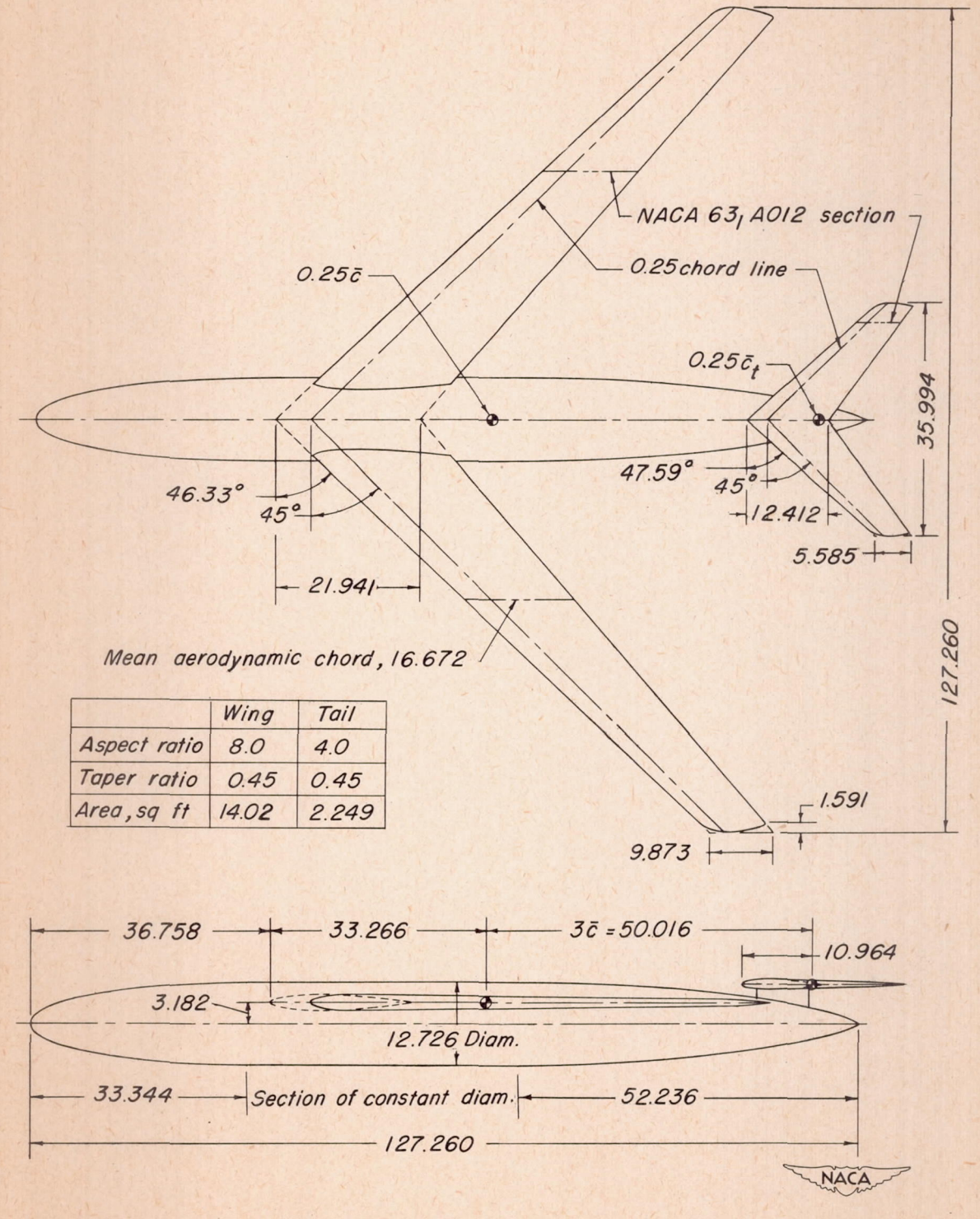

	Wing	Tail
Aspect ratio	8.0	4.0
Taper ratio	0.45	0.45
Area, sq ft	14.02	2.249

Figure 1.- Geometry of 45° sweptback wing of aspect ratio 8, fuselage and tail. All dimensions are in inches except where noted.

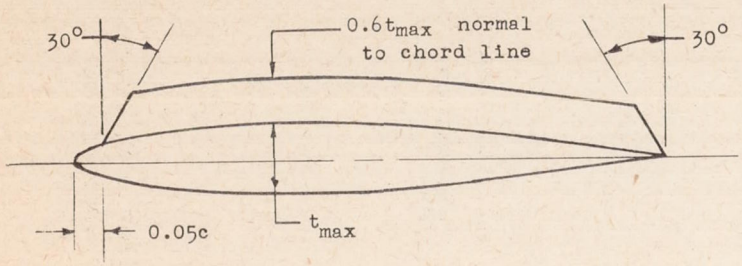

(a) Chord fence, located at 0.475, 0.575 and 0.800b/2.

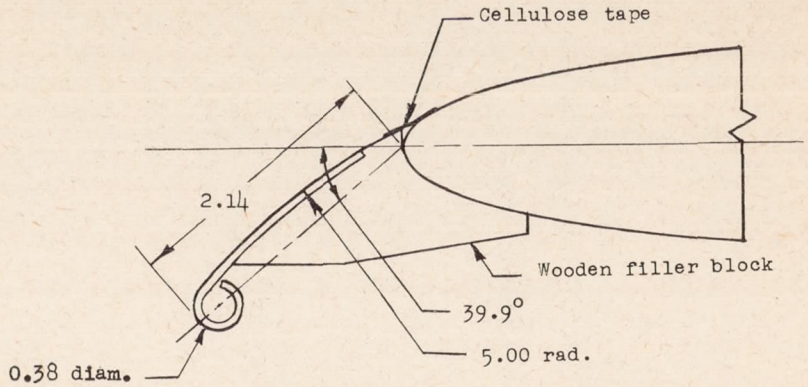

(b) Leading-edge flap extending from 0.50b/2 to 0.95b/2. This section is normal to the leading edge of the wing.

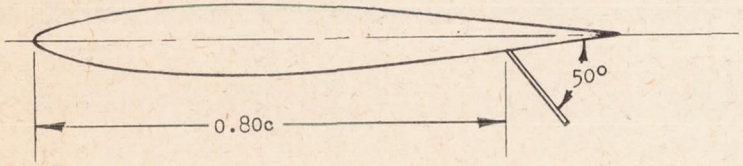

(c) Split flap extending from fuselage to 0.35b/2.

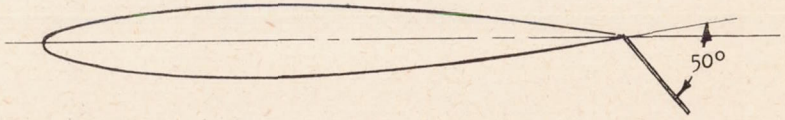

(d) Extended split flap extending from fuselage to 0.50b/2.

Figure 2.- Typical sections of high-lift and stall-control devices parallel to the plane of symmetry except where noted. Dimensions are in inches except where noted.

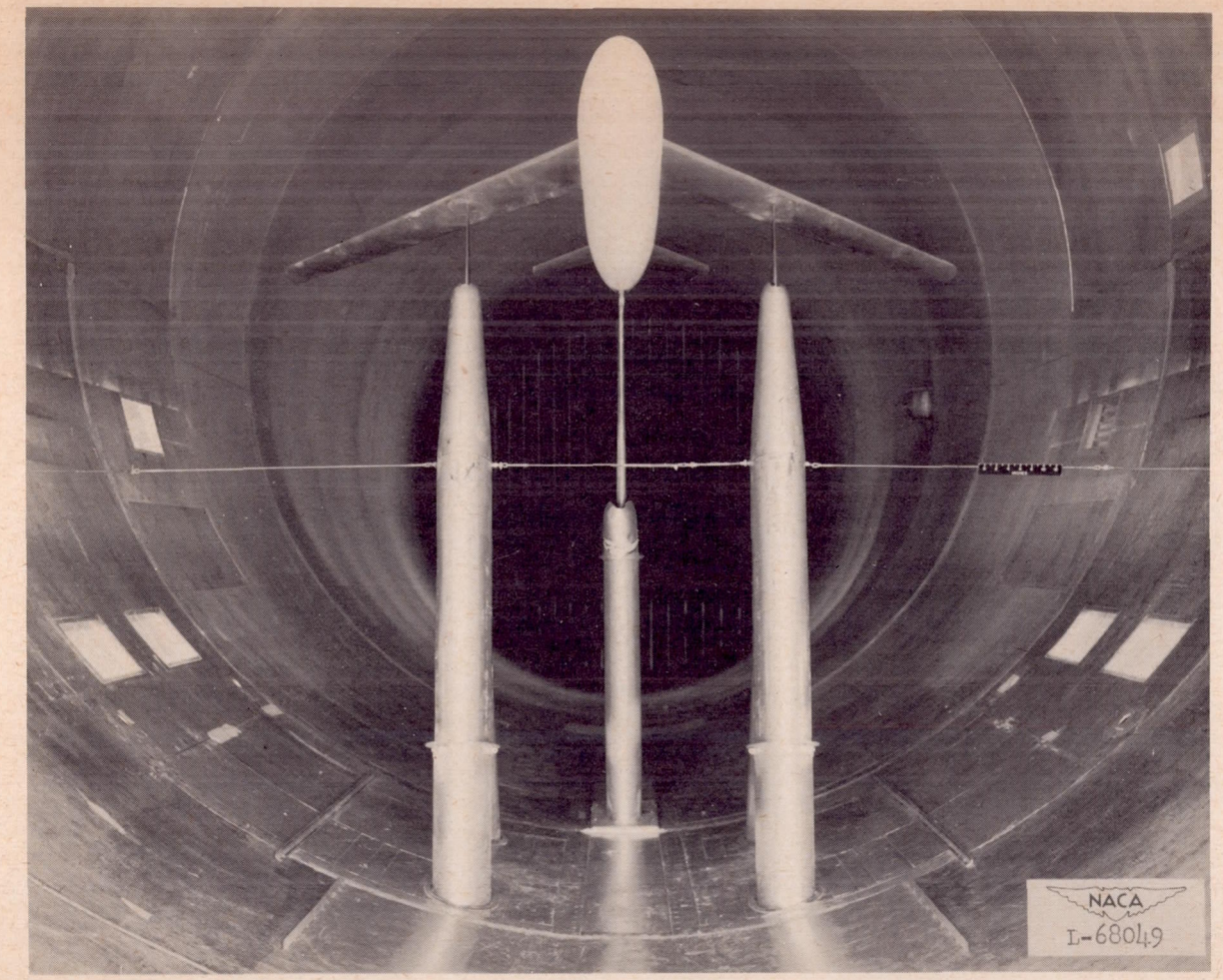

(a) Front view.

Figure 3.- The 45° sweptback-wing - fuselage combination with horizontal tail mounted in the 19-foot pressure tunnel.

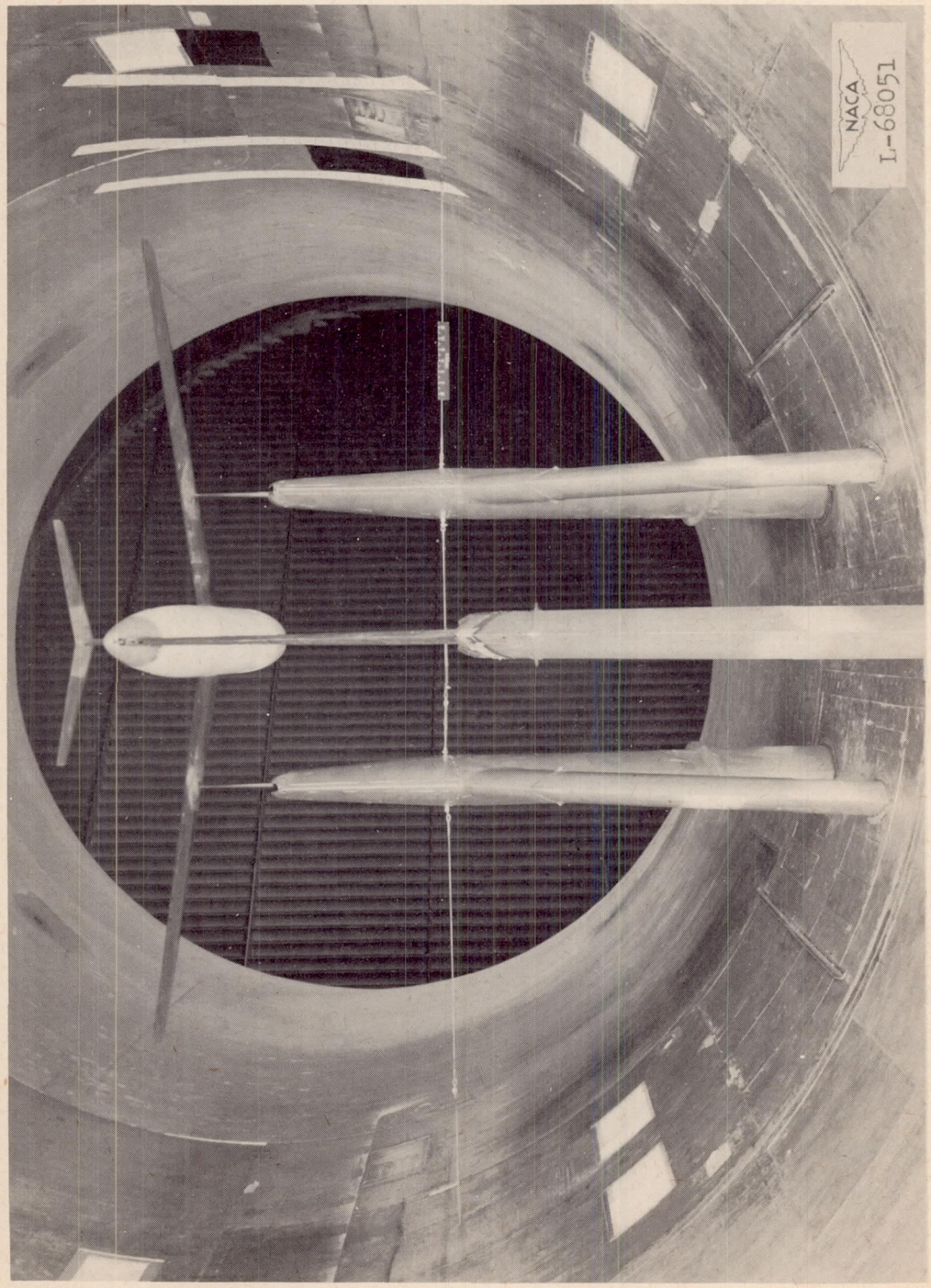

(b) Rear view.

Figure 3.- Concluded.

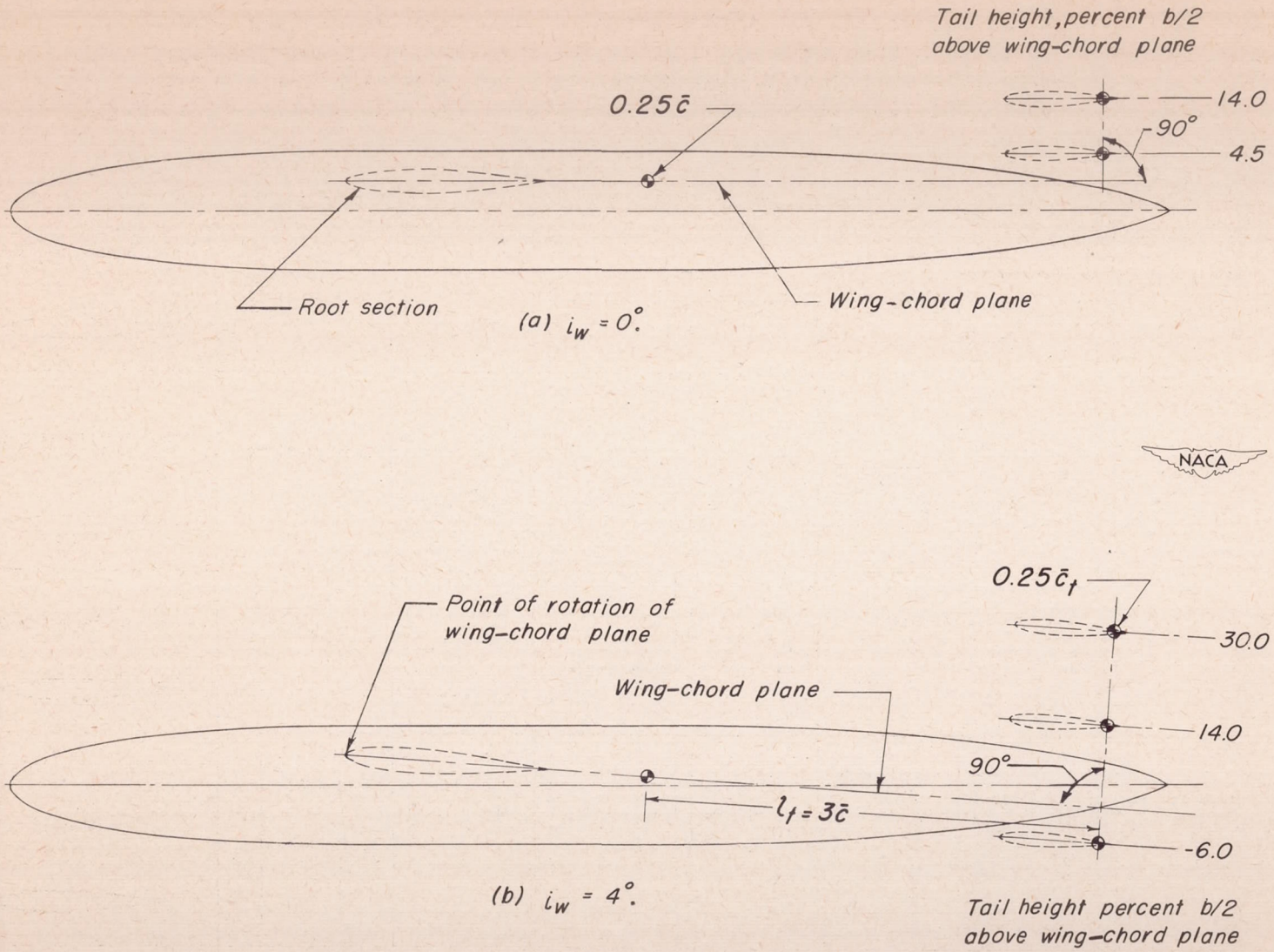

Figure 4.- Location of horizontal tail with respect to wing and fuselage.

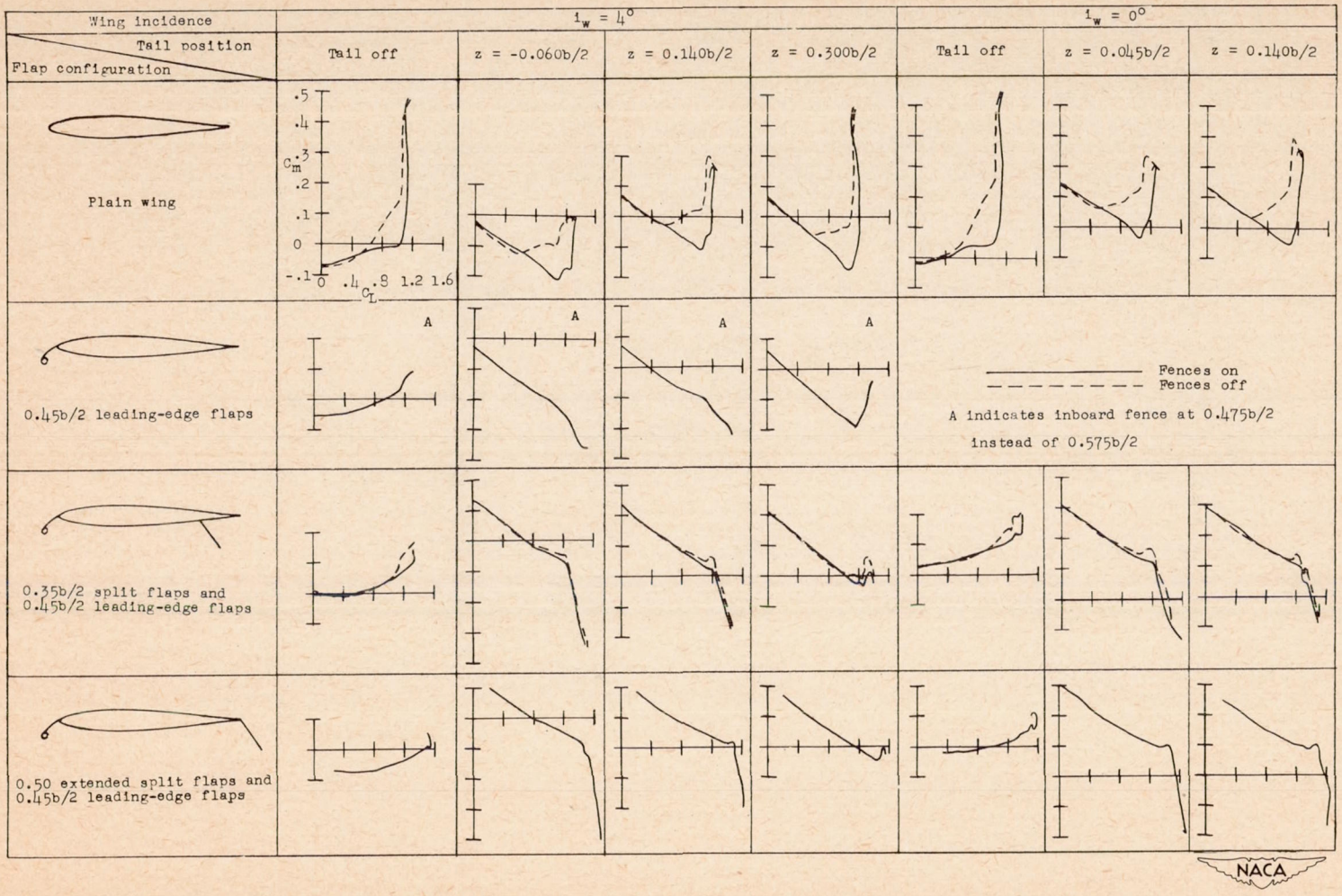

Figure 5.- Effect of a horizontal tail at various vertical locations on the pitching-moment characteristics for various flap configurations and two incidence wing angles on a 45° sweptback wing of aspect ratio 8.0. All tail-incidence angles are approximately -4°.

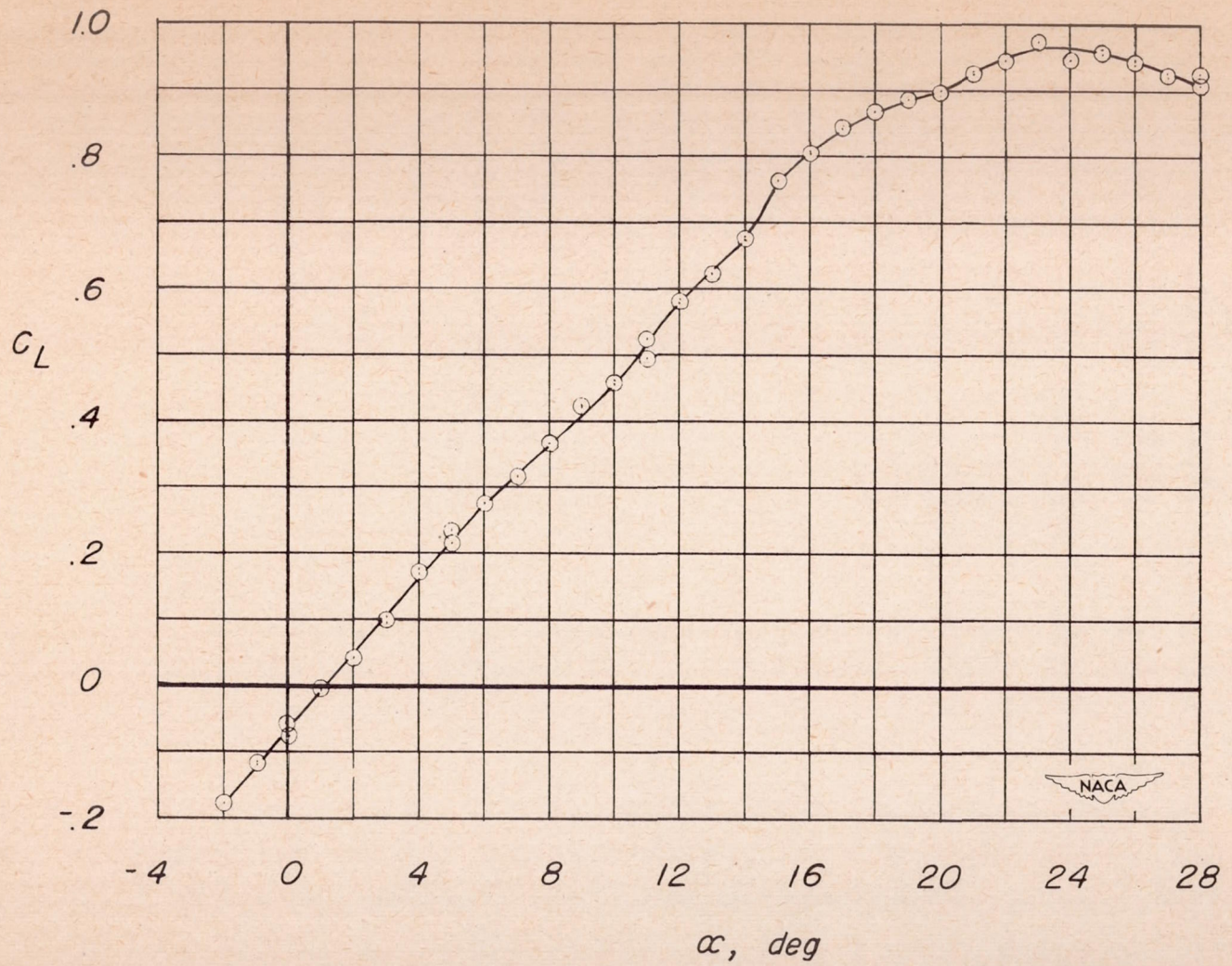

Figure 6.- Variation of lift coefficient with angle of attack of the 45° sweptback tail of aspect ratio 4.0 and NACA 63_1A012 airfoil sections. $R = 2.26 \times 10^6$ corresponding to the wing $R = 4.00 \times 10^6$.

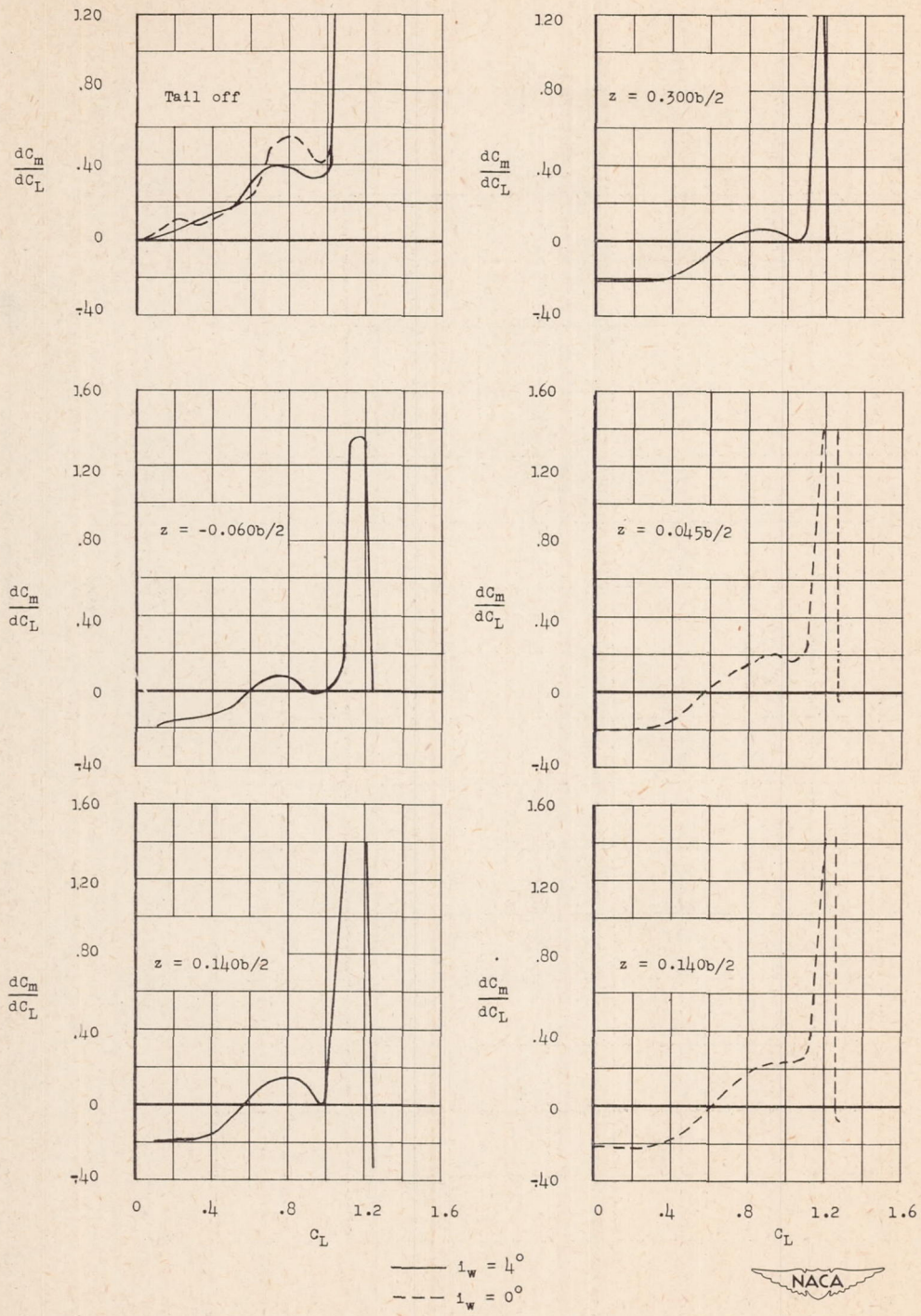

(a) Plain wing.

Figure 7.- Variation with lift coefficient of dC_m/dC_L for the wing-fuselage combination and dC_m/dC_L for $C_m = 0$ for the tail-on configurations. Center of gravity at $0.25\bar{c}$.

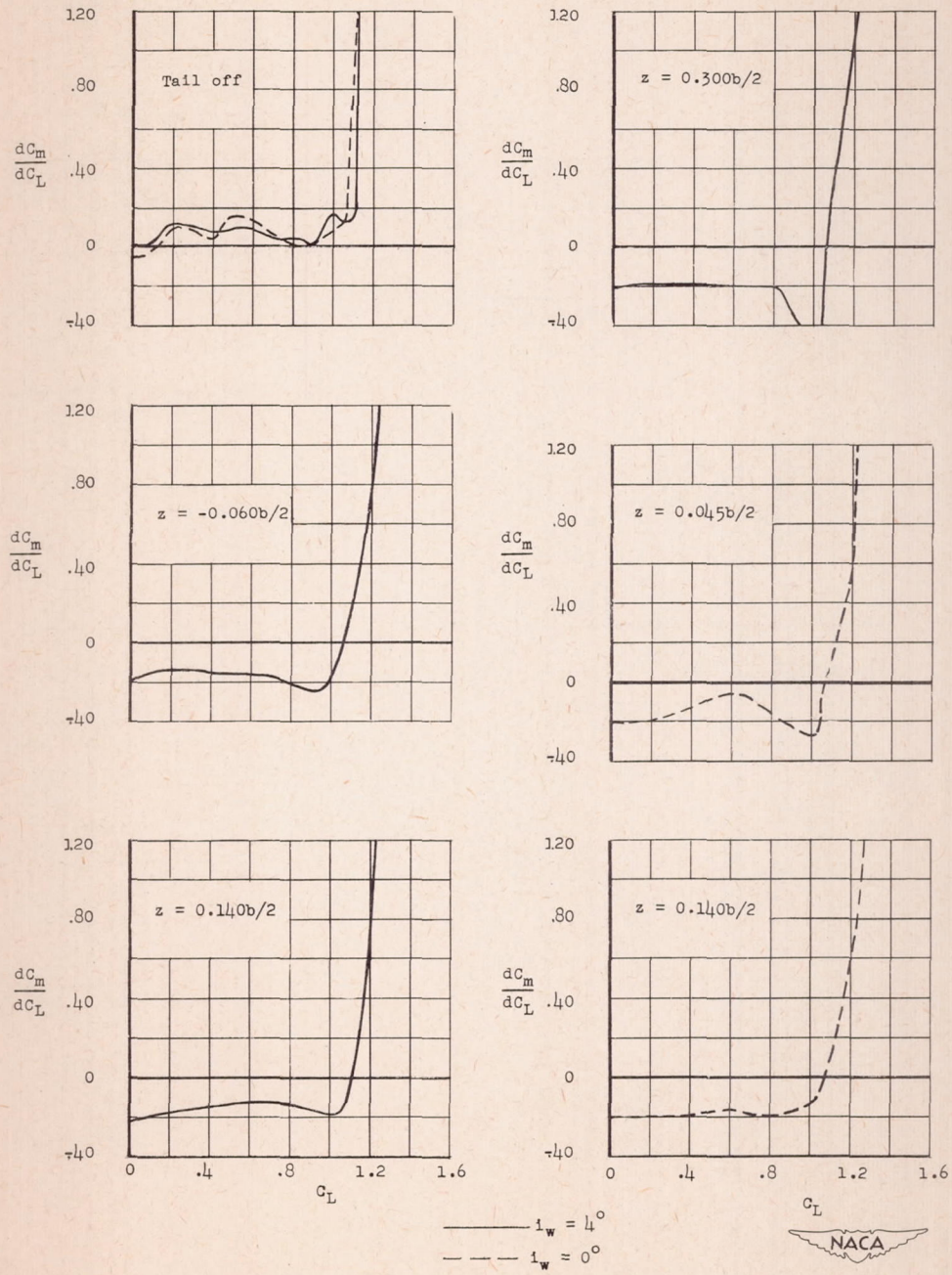

(b) 0.575b/2 and 0.800b/2 fences.

Figure 7.- Continued.

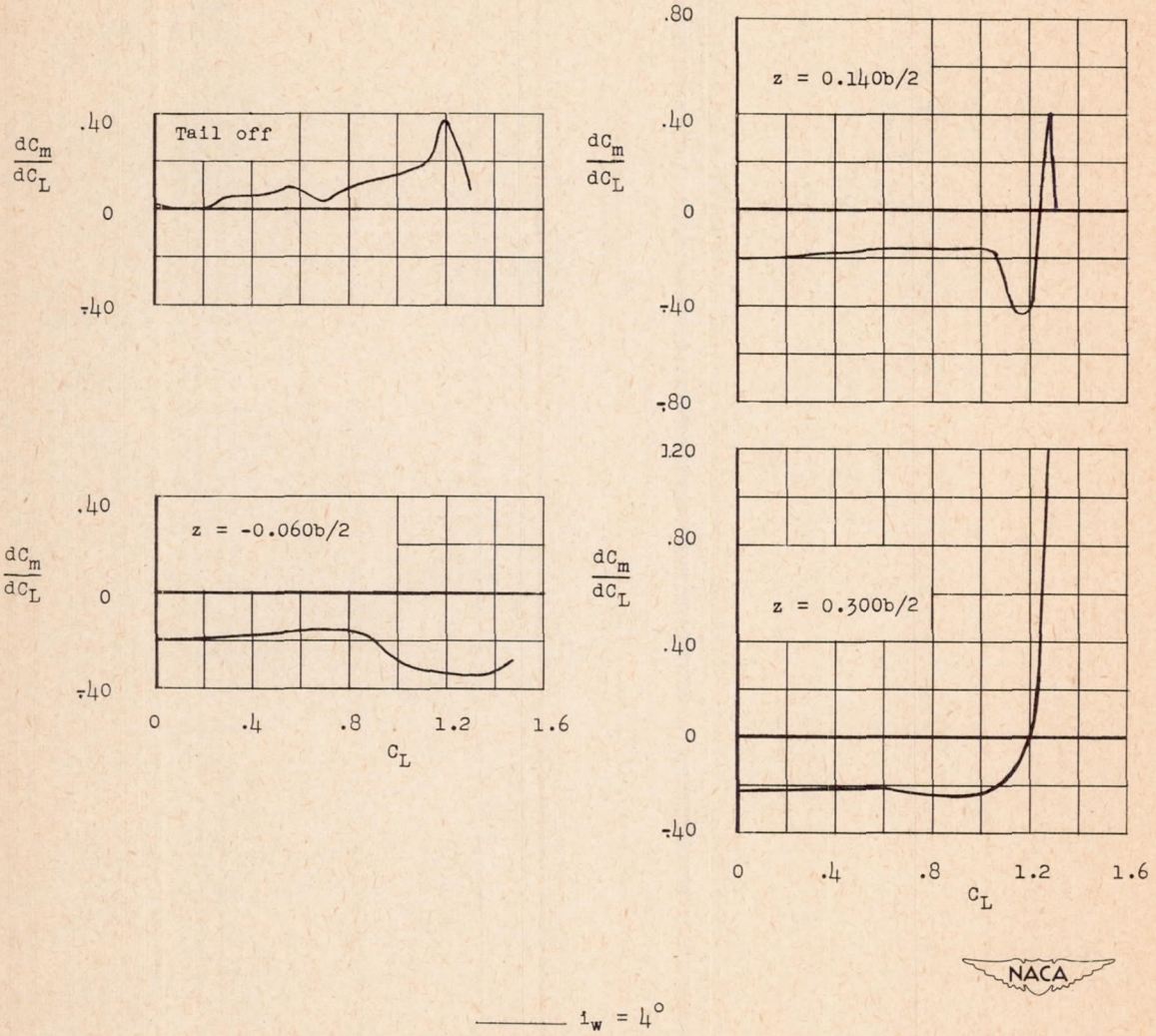

(c) 0.45b/2 leading-edge flaps and 0.475b/2 and 0.800b/2 fences.

Figure 7.- Continued.

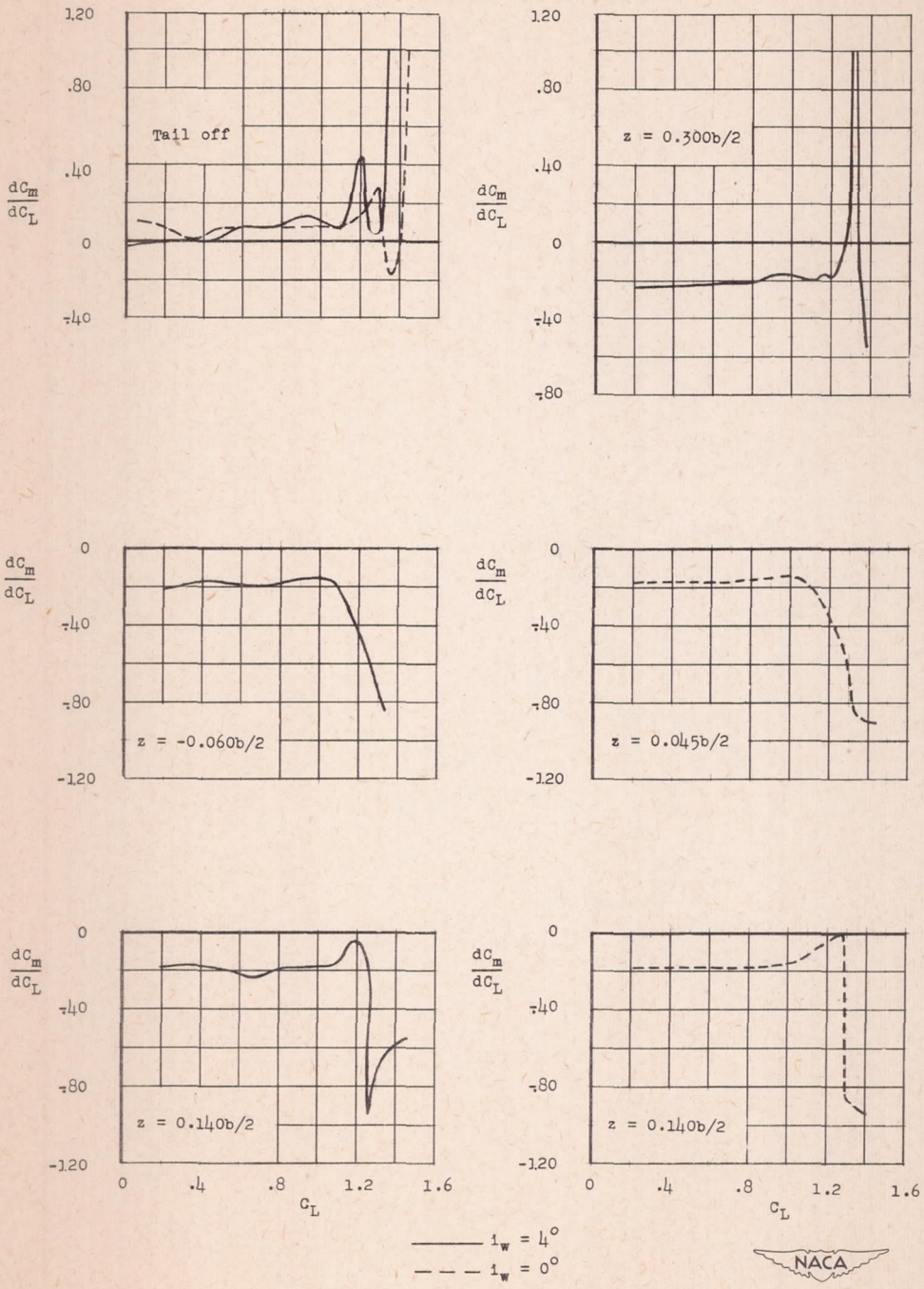

(d) 0.35b/2 split flaps, 0.45b/2 leading-edge flaps and 0.575b/2 and 0.800b/2 fences.

Figure 7.- Continued.

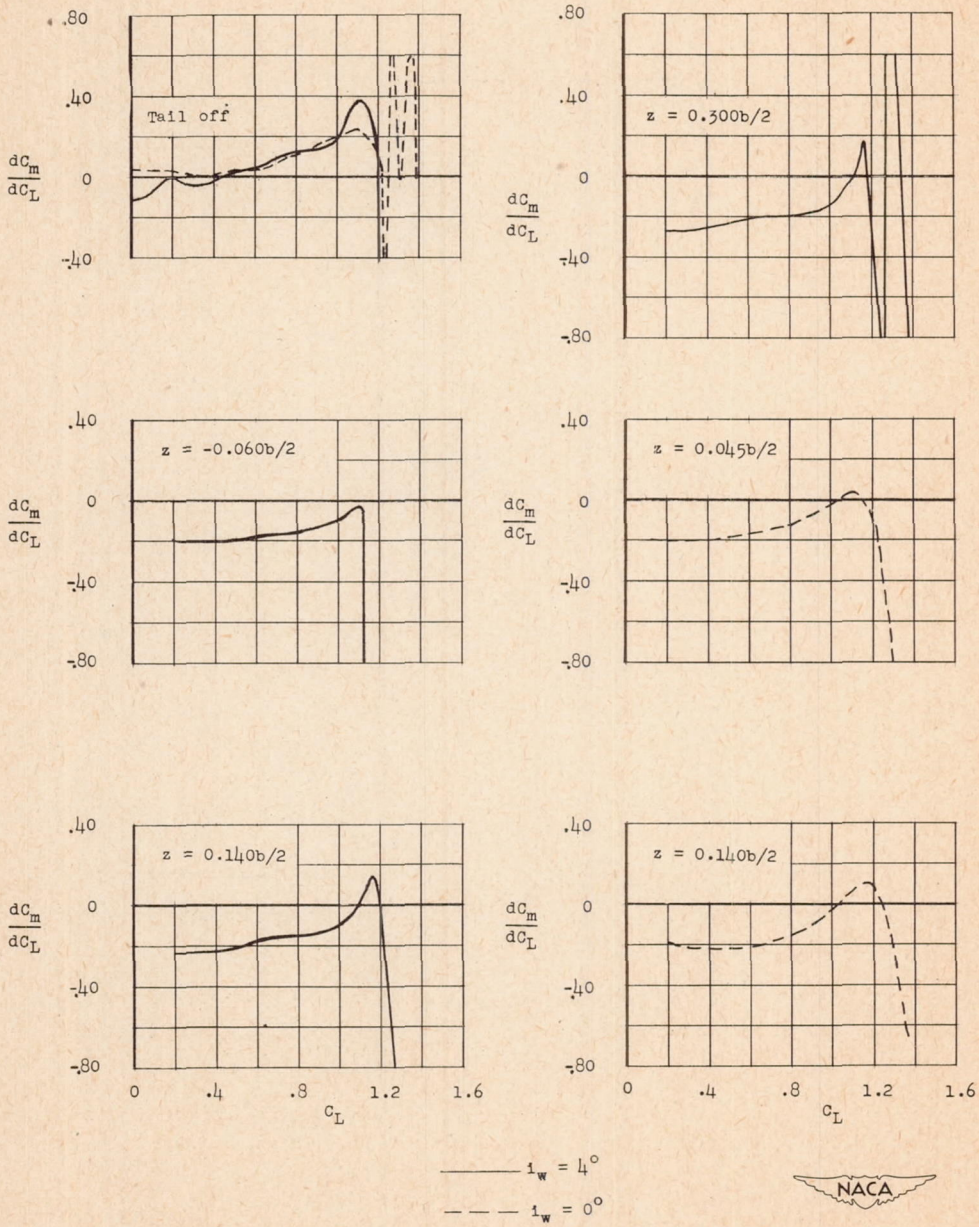

(e) 0.35b/2 split flaps and 0.45b/2 leading-edge flaps.

Figure 7.- Continued.

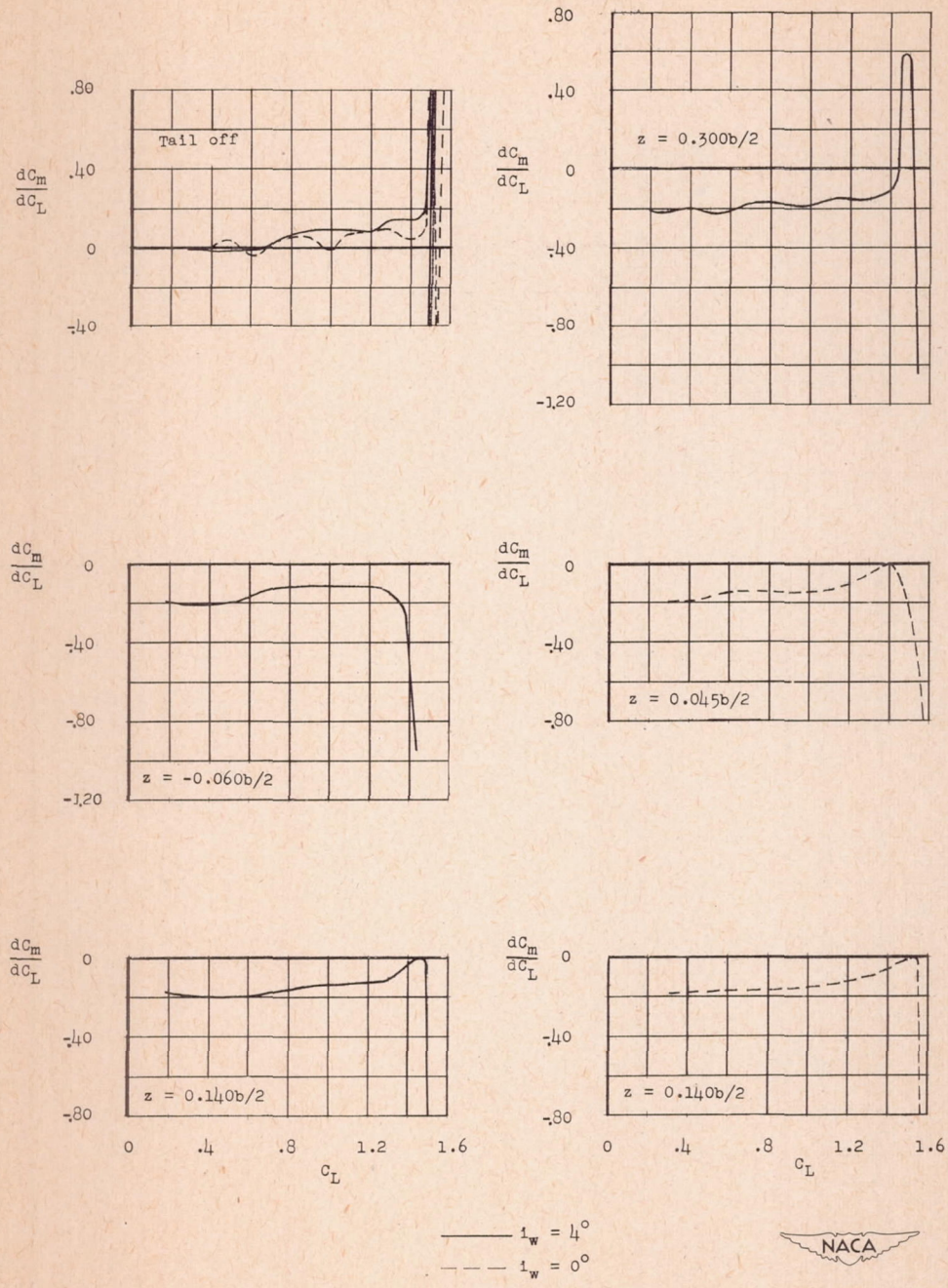

(f) 0.50b/2 extended split flaps, 0.45b/2 leading-edge flaps, and 0.575b/2 and 0.800b/2 fences.

Figure 7.- Concluded.

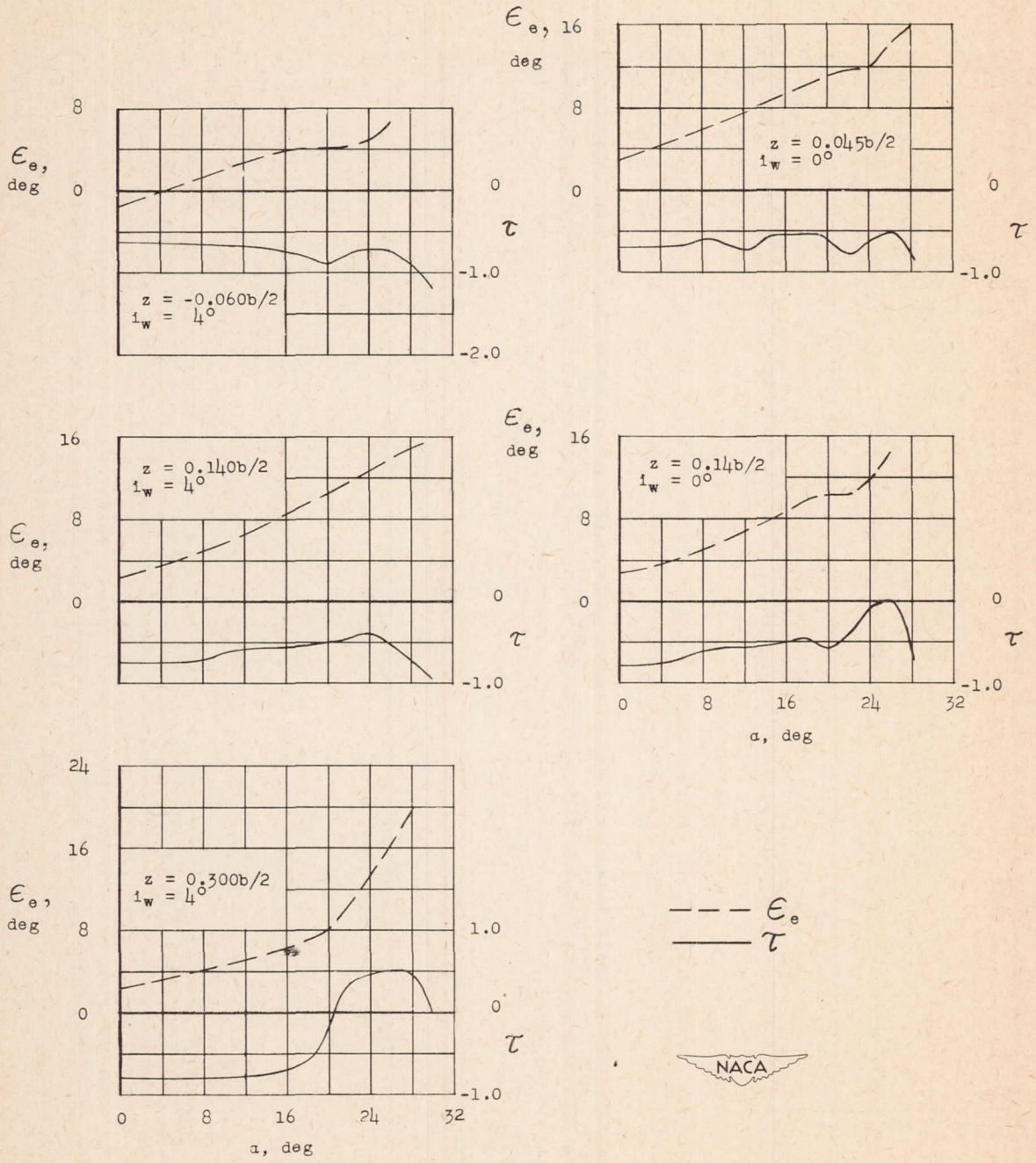

(a) Plain wing.

Figure 8.- Variation of tail effectiveness parameter τ and the effective downwash angle ϵ_e with angle of attack.

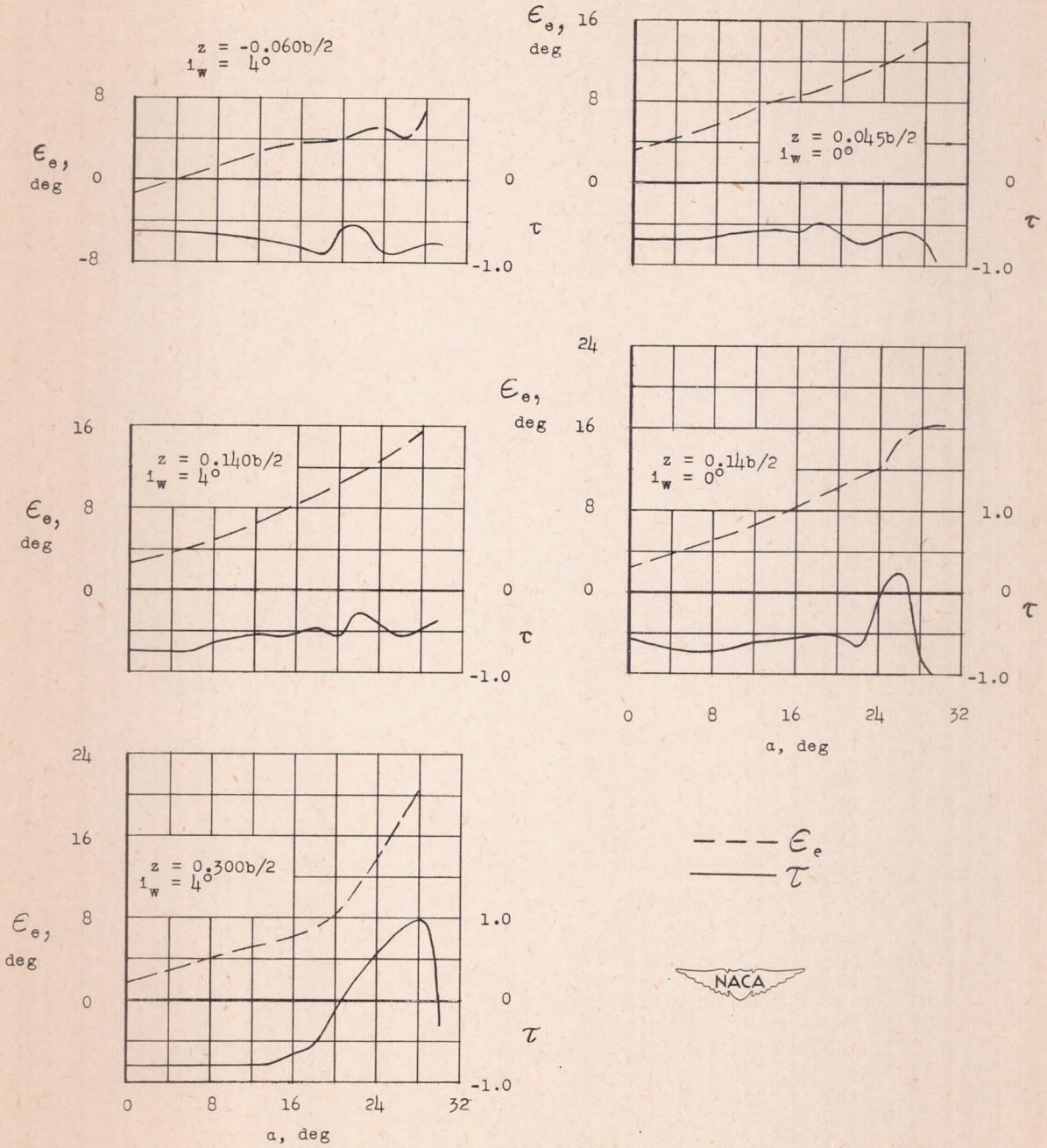

(b) 0.575b/2 and 0.800b/2 fences.

Figure 8.- Continued.

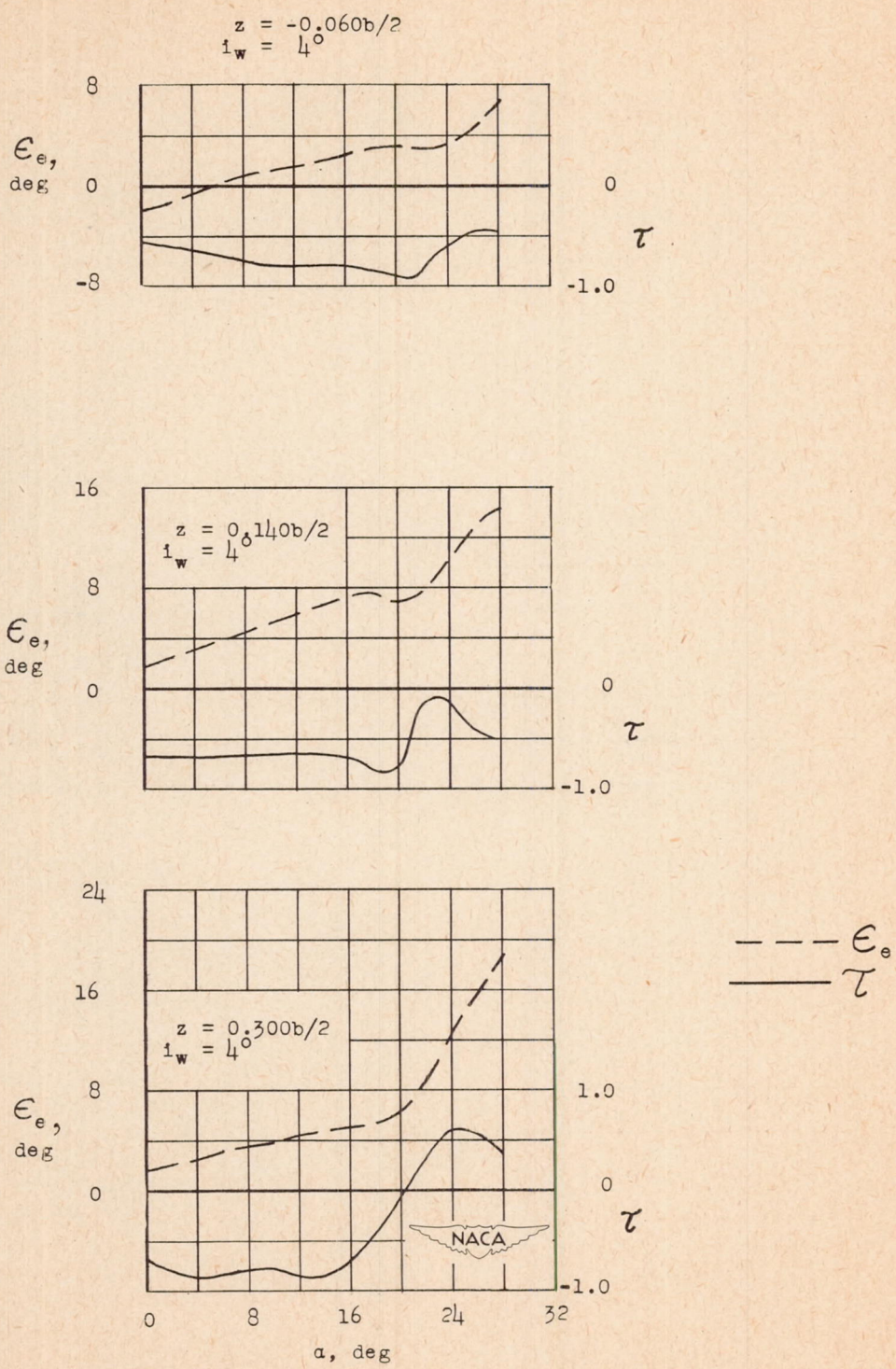

(c) 0.45b/2 leading-edge flaps and 0.475b/2 and 0.800b/2 fences.

Figure 8.- Continued.

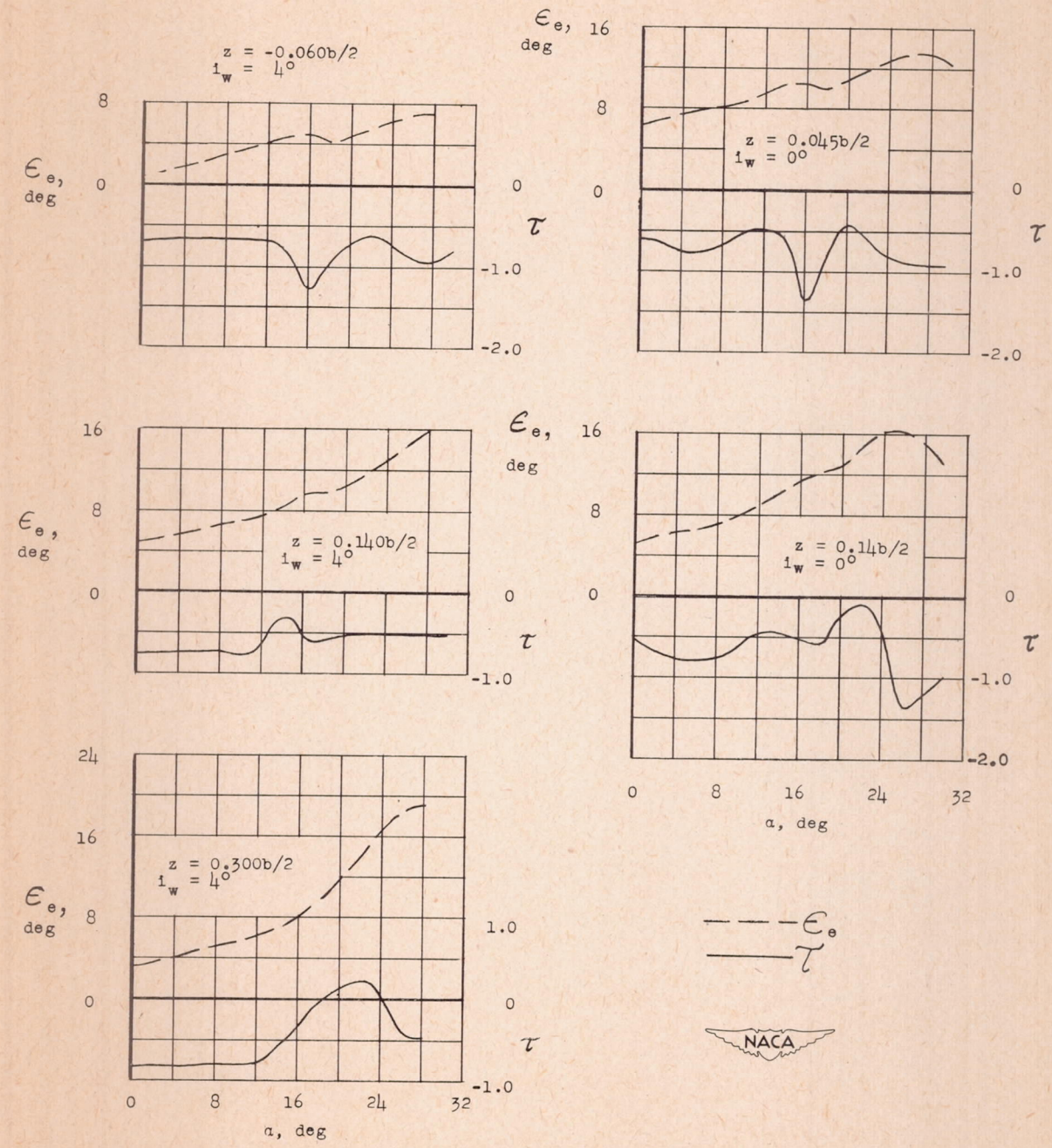

(d) 0.35b/2 split flaps, 0.45b/2 leading-edge flaps and 0.575b/2 and 0.800b/2 fences.

Figure 8.- Continued.

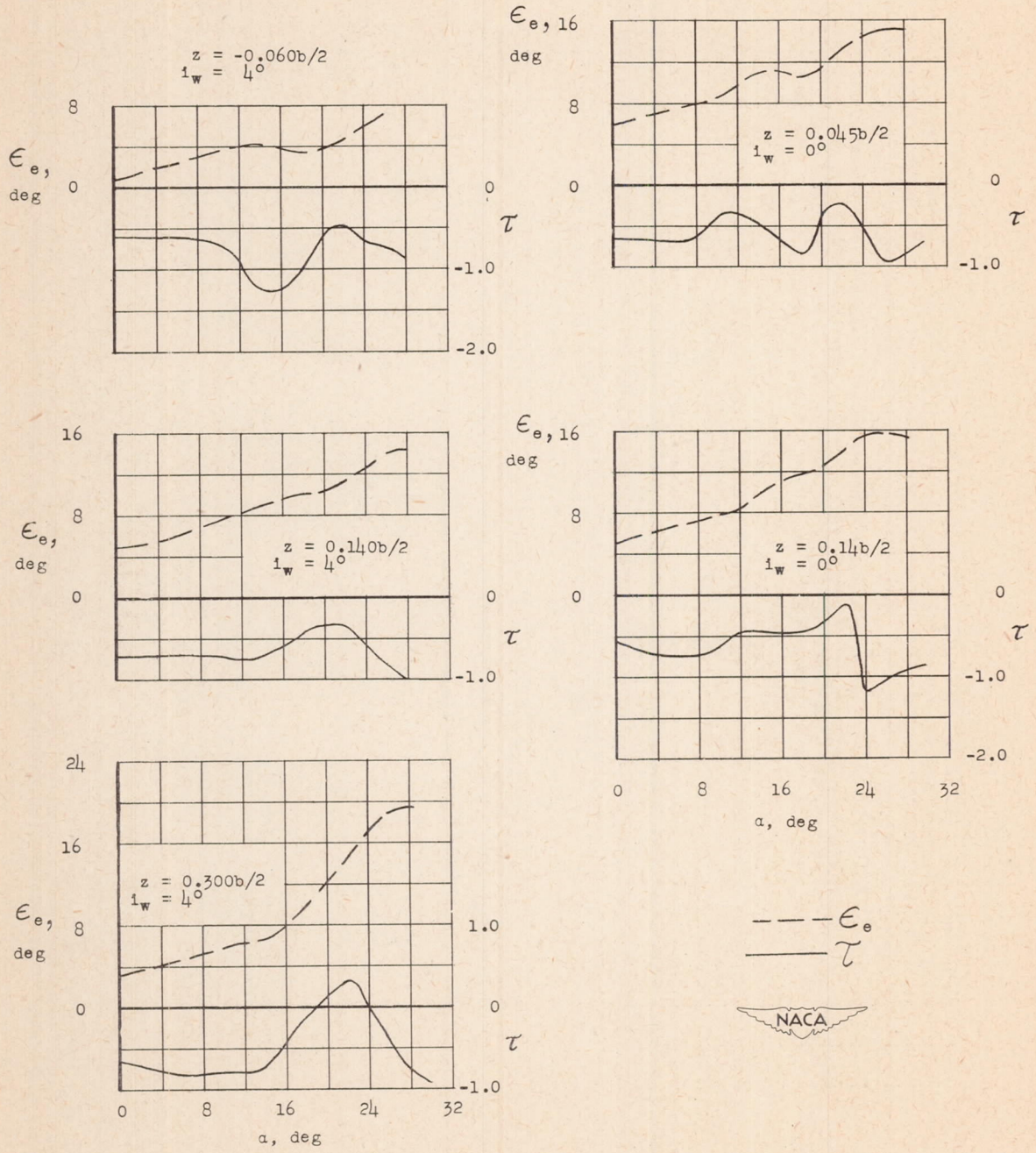

(e) 0.35b/2 split flaps and 0.45b/2 leading-edge flaps.

Figure 8.- Continued.

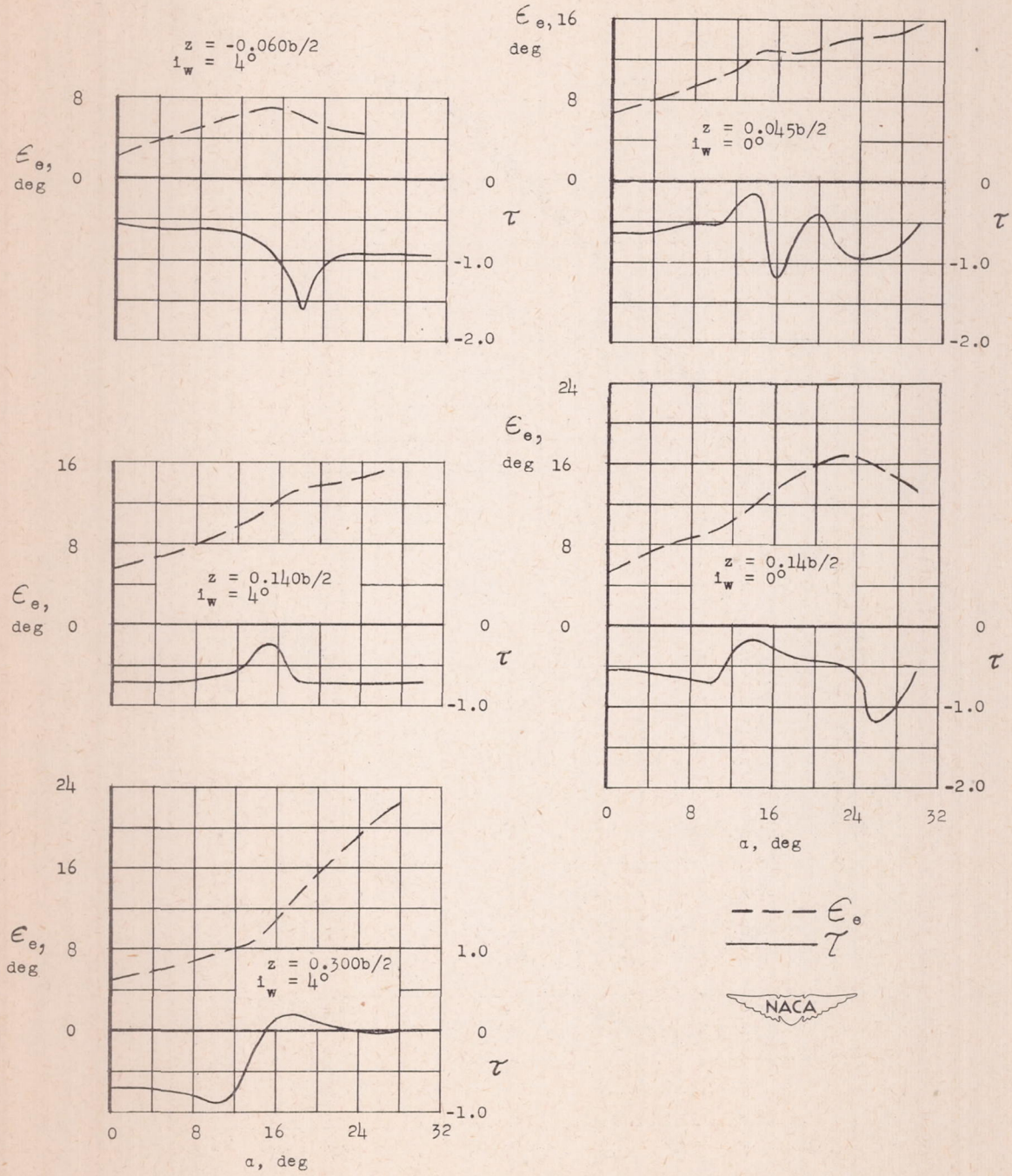

(f) 0.50b/2 extended split flaps, 0.45b/2 leading-edge flaps and 0.575b/2 and 0.800b/2 fences.

Figure 8.- Concluded.

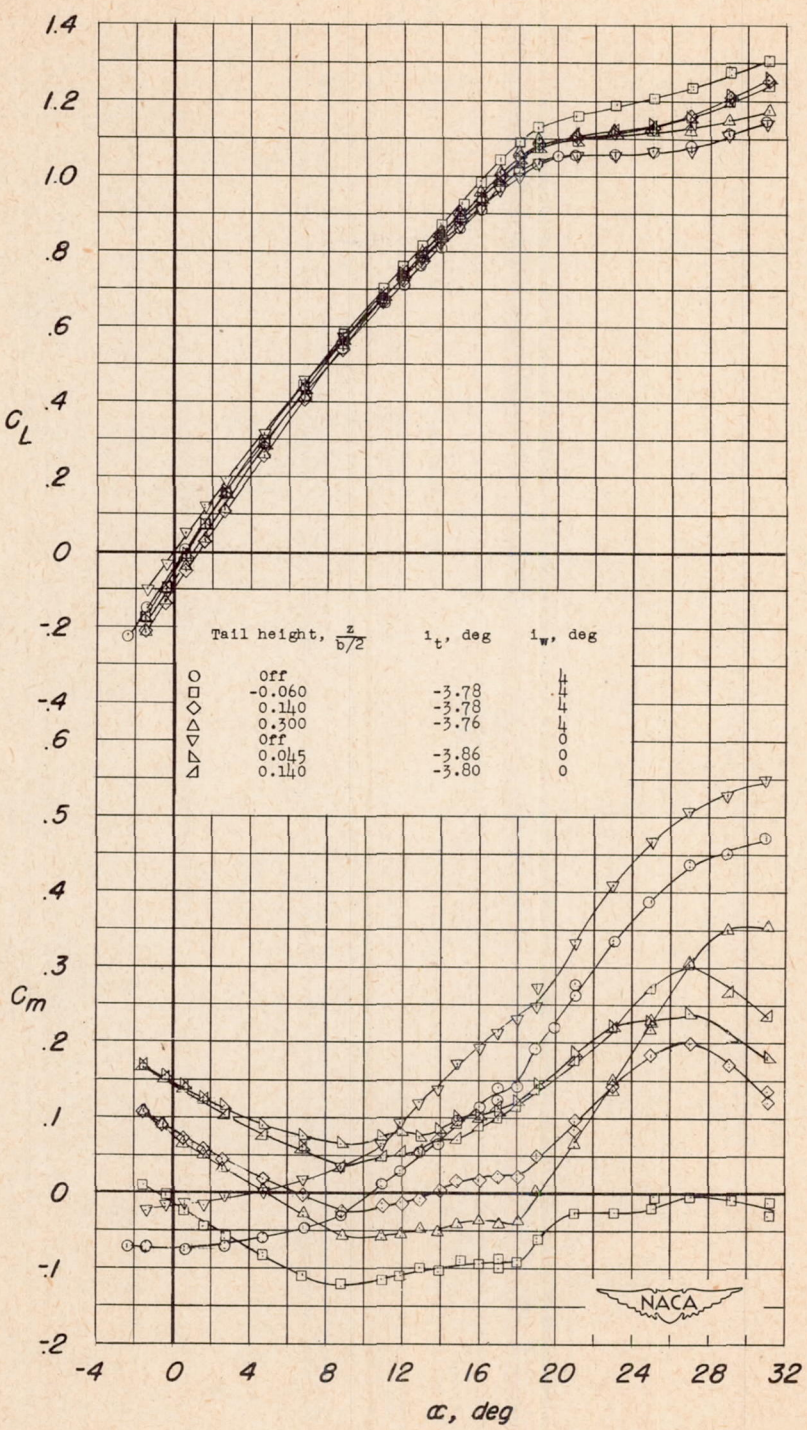

(a) Plain wing.

Figure 9.- Variation of lift coefficient and pitching-moment coefficient with angle of attack for various tail locations and two wing-incidence angles.

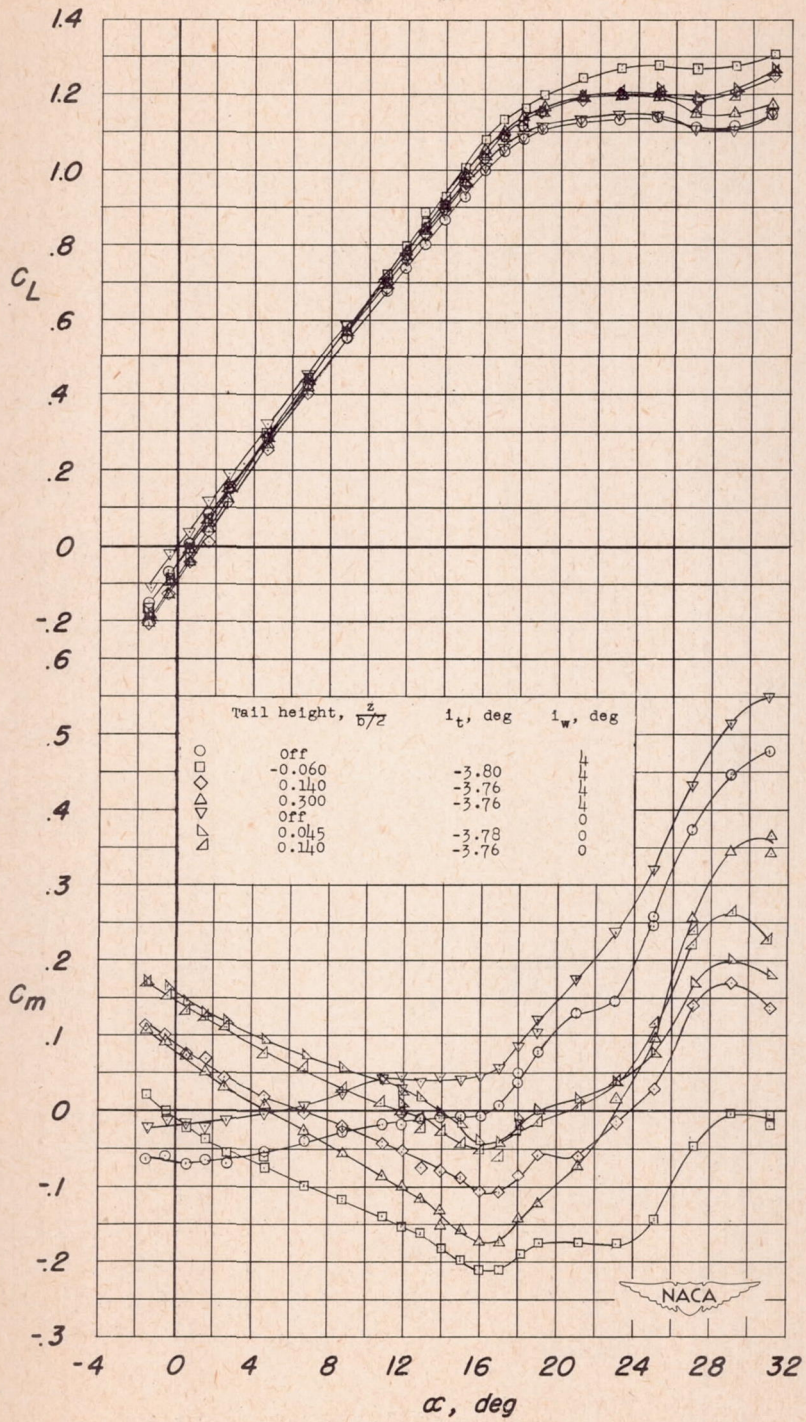

(b) 0.575b/2 and 0.800b/2 fences.

Figure 9.- Continued.

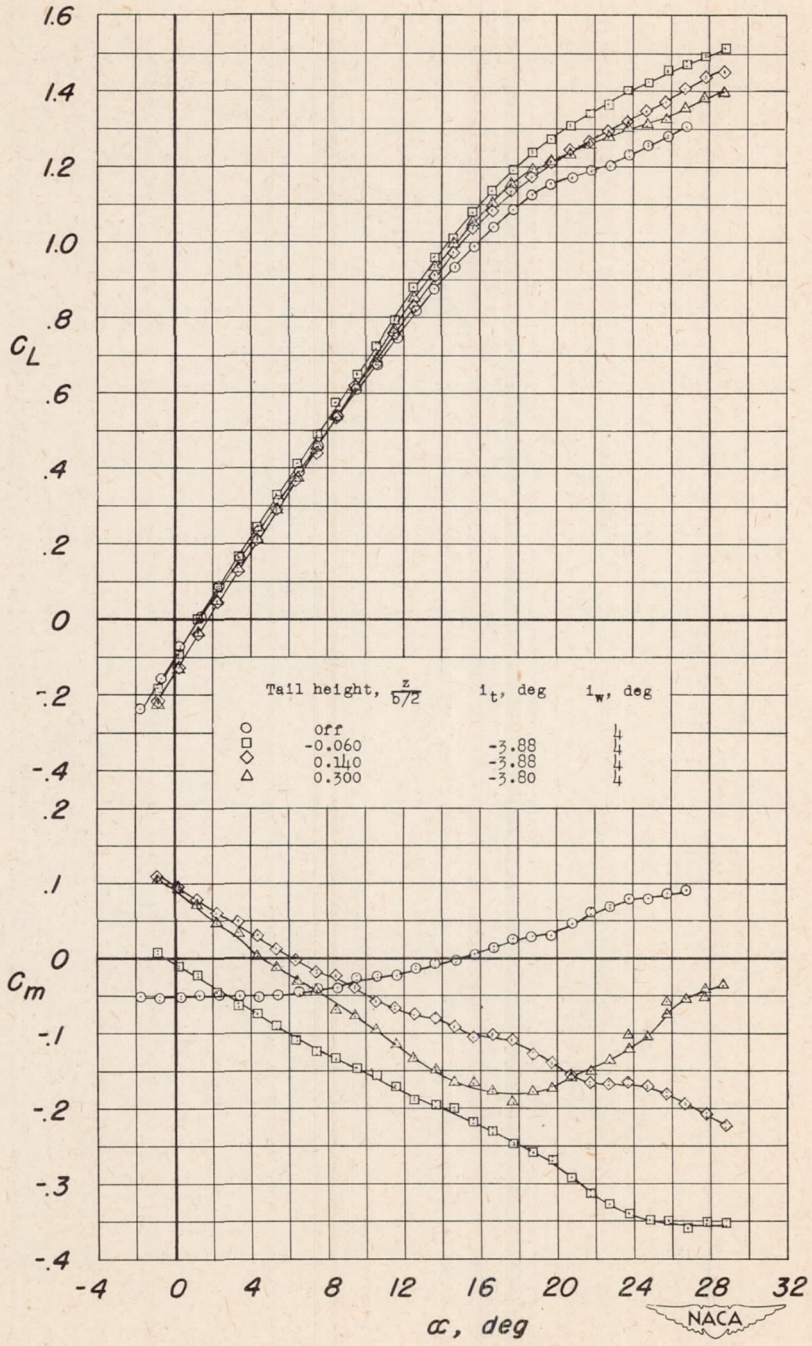

(c) 0.45b/2 leading-edge flaps and 0.475b/2 and 0.800b/2 fences.

Figure 9.- Continued.

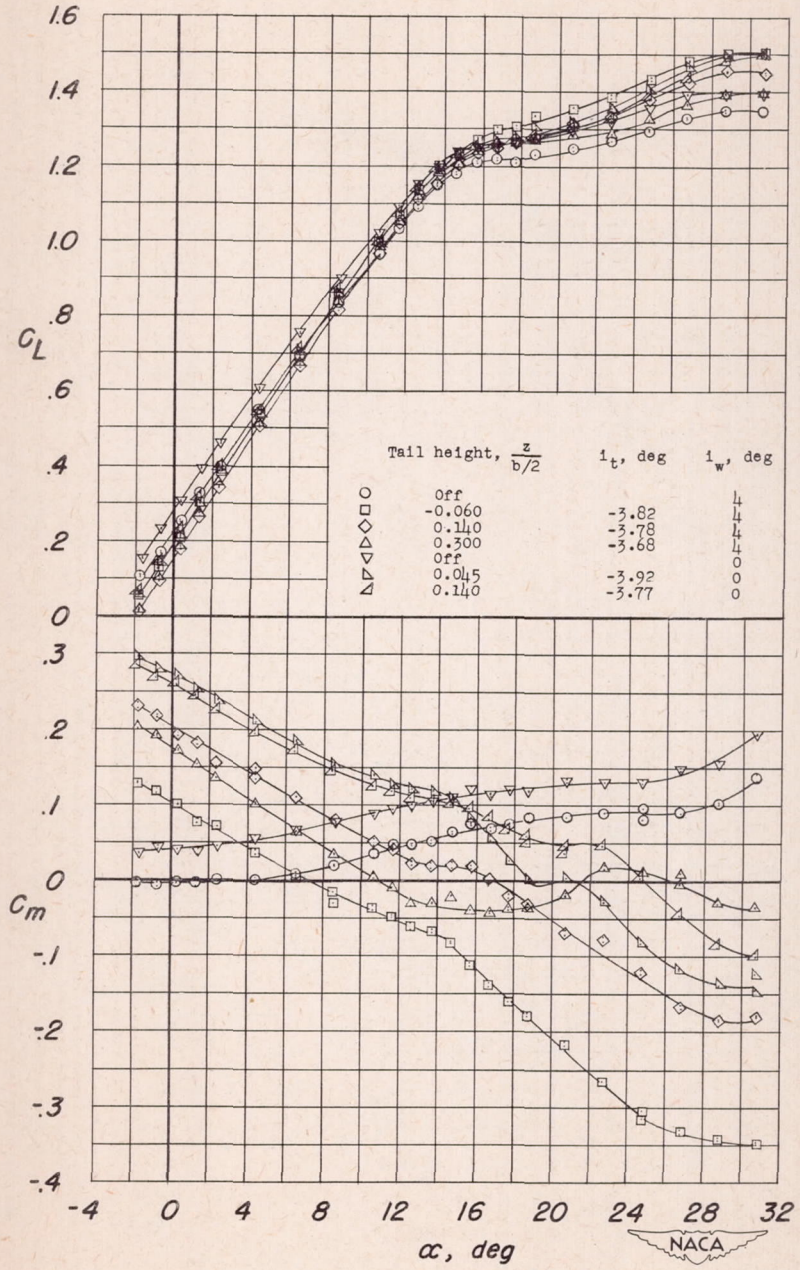

(d) 0.35b/2 split flaps, 0.45b/2 leading-edge flaps, and 0.575b/2 and 0.800b/2 fences.

Figure 9.- Continued.

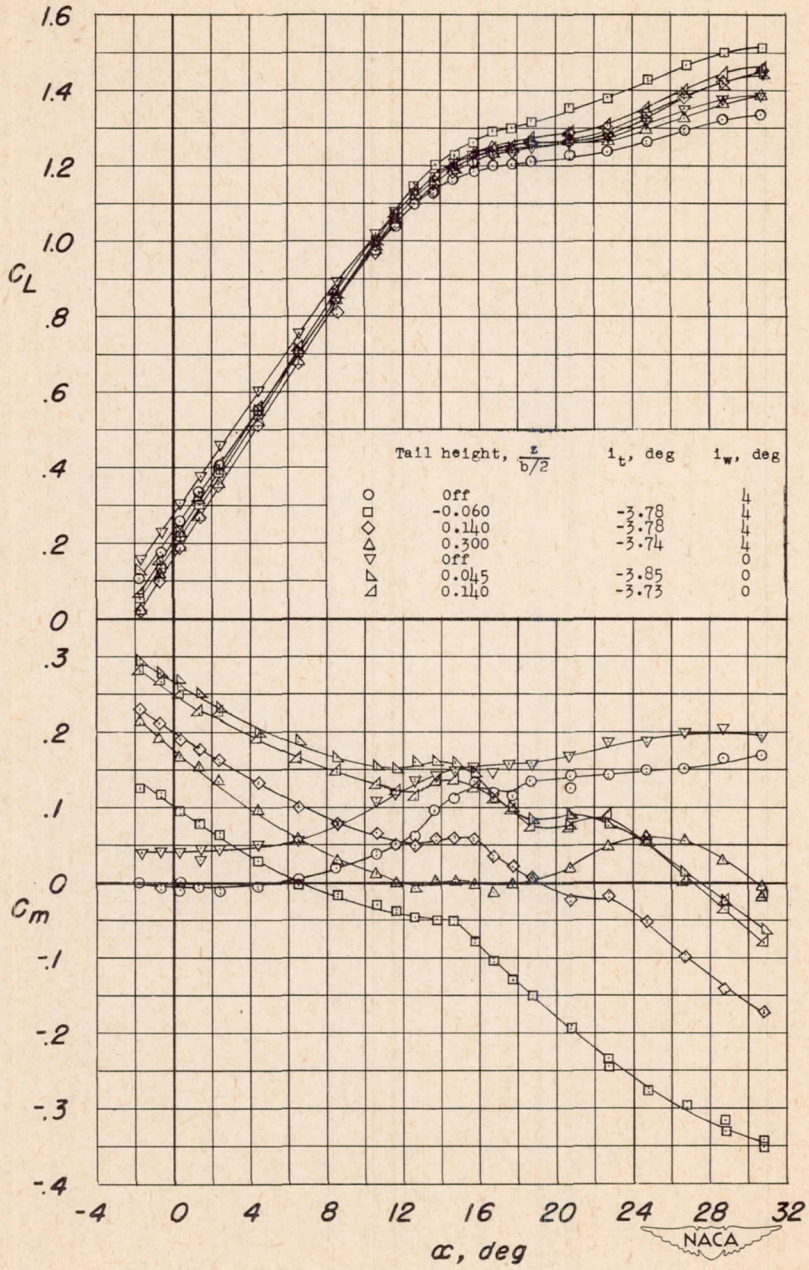

(e) 0.35b/2 split flaps and 0.45b/2 leading-edge flaps.

Figure 9.- Continued.

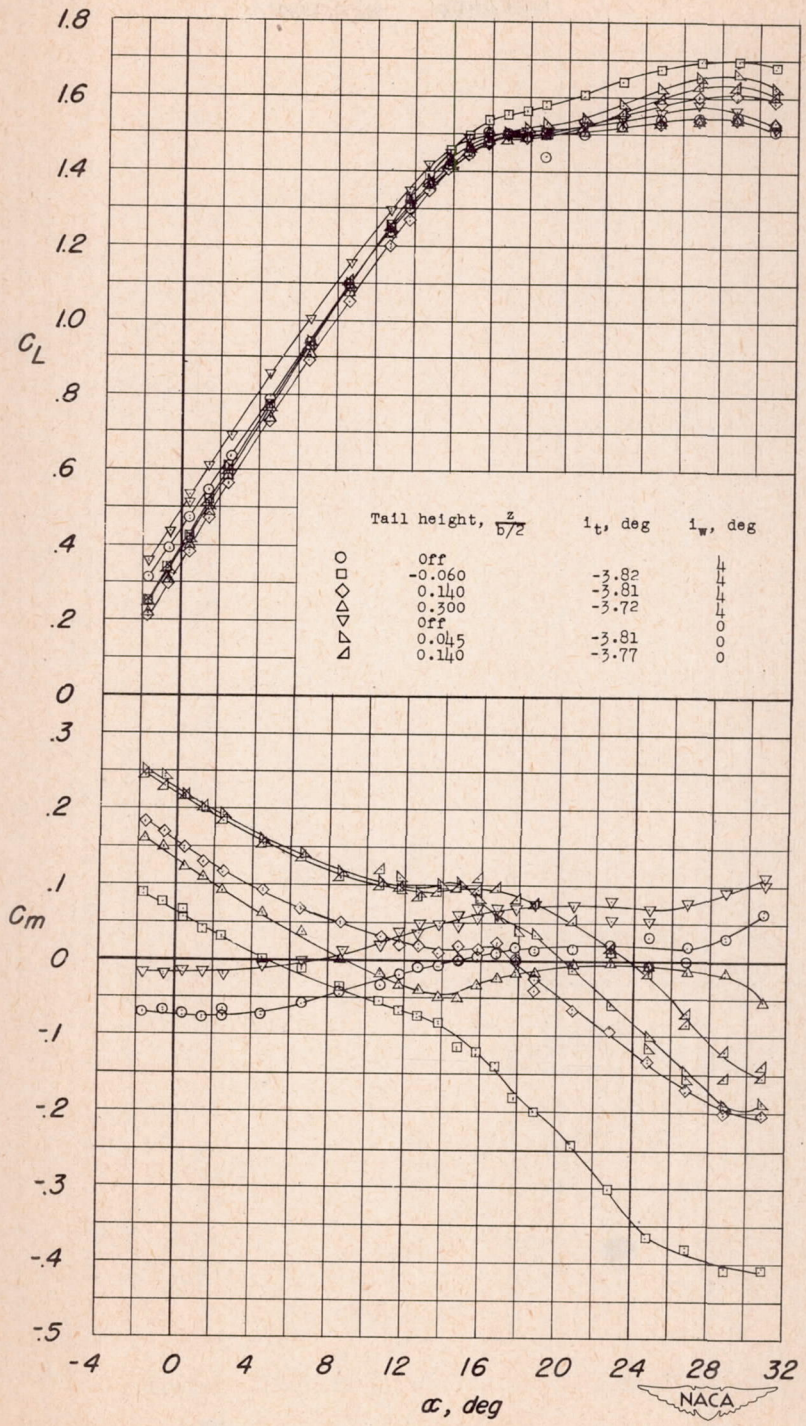

(f) 0.50b/2 extended split flaps, 0.45b/2 leading-edge flaps and 0.575b/2 and 0.800b/2 fences.

Figure 9.- Concluded.

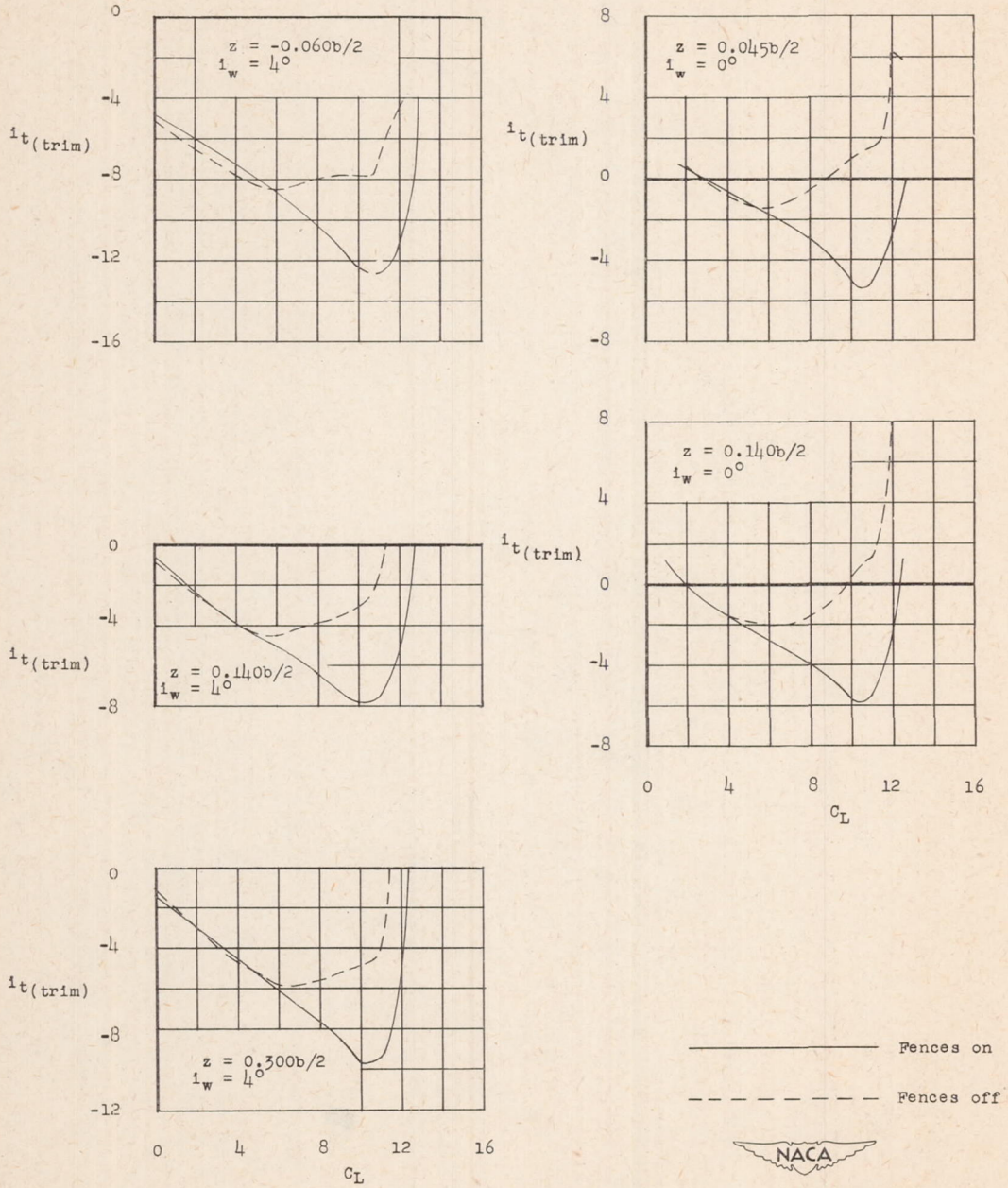

(a) Plain wing with and without fences.

Figure 10.- Variation with lift coefficient of the tail-incidence angle required for trim. Center of gravity at 0.25$\bar{c}$.

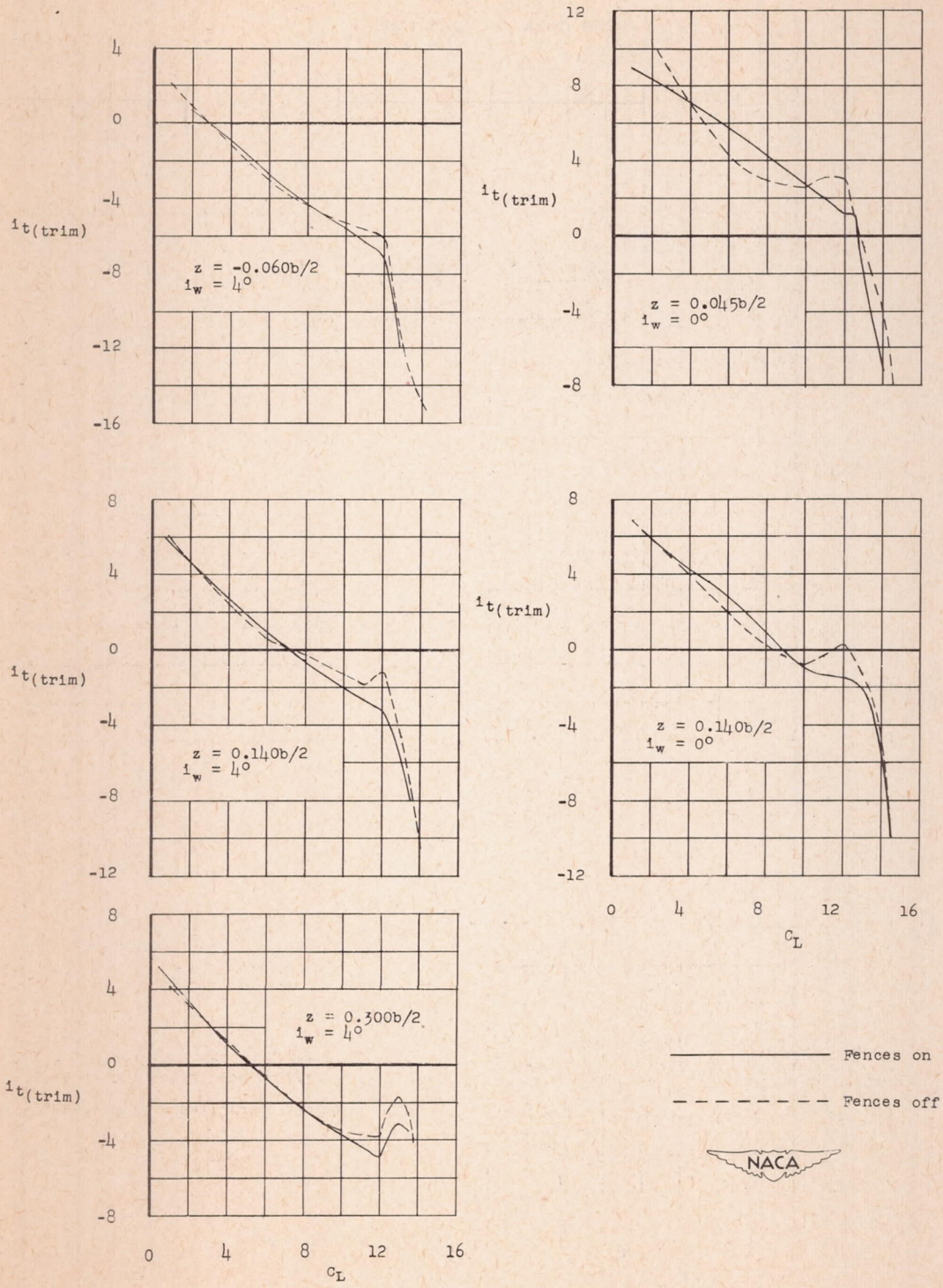

(b) 0.35b/2 split flaps and 0.45b/2 leading-edge flaps with and without fences.

Figure 10.- Continued.

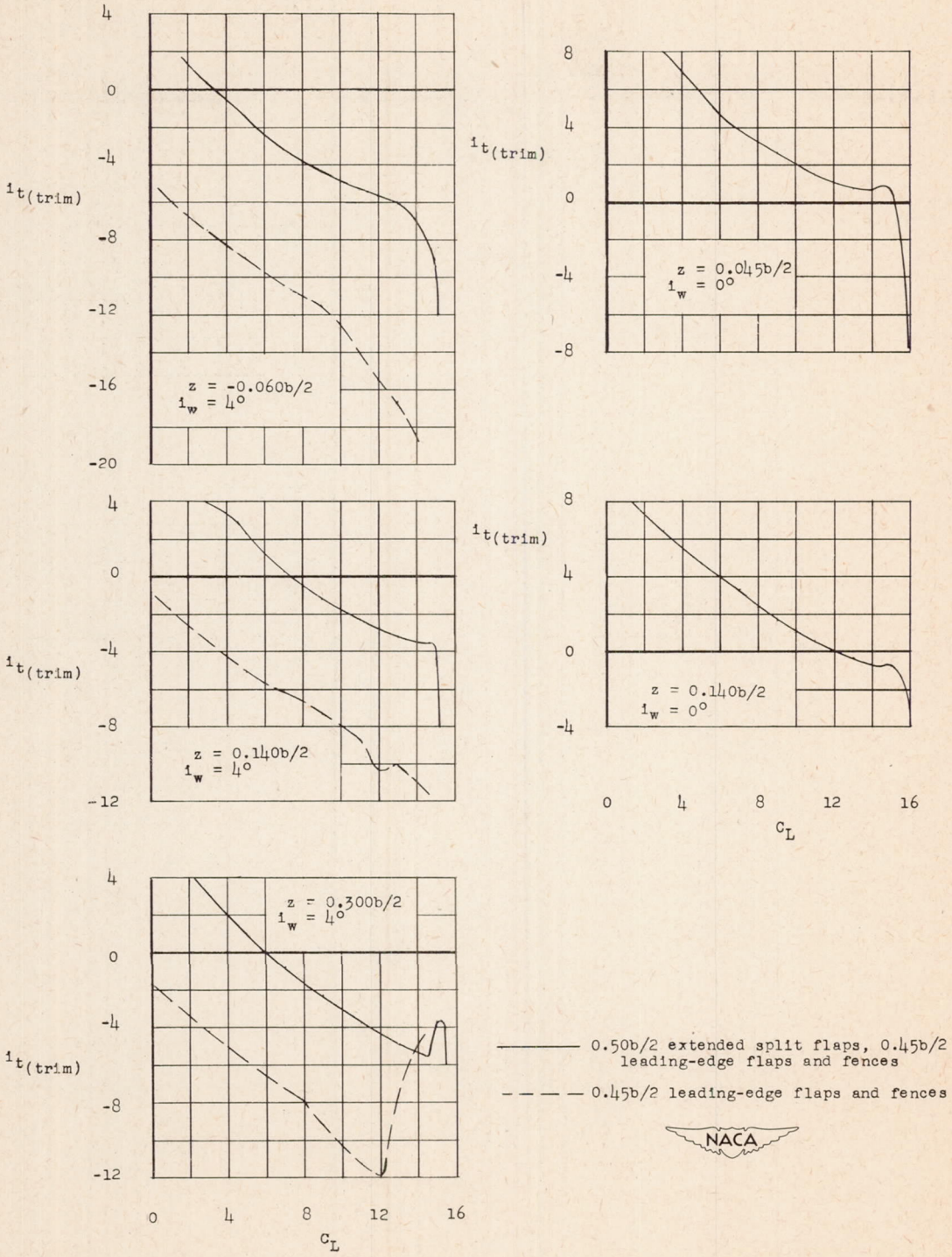

(c) 0.50b/2 extended split flaps plus 0.45b/2 leading-edge flaps and fences, and 0.45b/2 leading-edge flaps plus fences.

Figure 10.- Concluded.

NACA-Langley - 1-21-52 - 325